Sedimentary Geology 420 (2021) 105904

Contents lists available at ScienceDirect

Sedimentary Geology

journal homepage: www.elsevier.com/locate/sedgeo

Middle Triassic carbonates of Eastern Iberia (Western Tethyan Realm): A shallow platform model

Alberto Pérez-López [a,b,*], Constantino Benedicto [c], Federico Ortí [d]

[a] Departamento de Estratigrafía y Paleontología, Facultad de Ciencias, Avda. Fuentenueva, 18071 Granada, Spain
[b] Instituto Andaluz de Ciencias de la Tierra (CSIC-Universidad de Granada), Avda. de las Palmeras, 4, 18100 Armilla, Granada, Spain
[c] Ilustre Colegio Oficial de Geólogos (ICOG), 7557, C/ El Castillo 83 bajo, 12429 El Toro, Castelló de la Plana, Spain
[d] Departament de Mineralogia, Petrologia i Geologia aplicada, Facultat de Ciències de la Terra, Universitat de Barcelona (UB), C/ Martí Franquès s/n, 08028 Barcelona, Spain

ARTICLE INFO

Article history:
Received 10 February 2021
Received in revised form 2 April 2021
Accepted 3 April 2021
Available online 20 April 2021

Editor: Dr. Brian Jones

Keywords:
Epicontinental platform
Muschelkalk
Carbonate sedimentology
Rimmed shelf
Carbonate ramp
Facies

ABSTRACT

Much of the eastern sector of the Mesozoic Iberian basin belongs to the 'Mediterranean type' Triassic. This type is characterized by a Middle Triassic stratigraphic record comprised of two carbonate Muschelkalk units (lower and upper) separated by a detrital-evaporite middle Muschelkalk unit. In the present study areas, the two first marine flooding episodes of the Middle Triassic led to the deposition of extensive shallow-water carbonates on a block-controlled epicontinental platform in the lower and upper Muschelkalk units. These carbonates were part of third-order transgressive–regressive sequences. The two carbonate sequences display similar vertical facies and stratigraphic sub-unit arrangements. The base of the two sequences is marked by a (lower) carbonate-marl alternation, which was deposited in mixed tidal flat-to-lagoon settings. In the middle of the sequences, the carbonate character is predominant and facies associations mainly suggest shallow waters and high environmental variability. The change from a transgressive to regressive trend occurs in the middle of the sequences, although the position of the maximum flooding zone can vary from one to another stratigraphic section. The tops of the sequences show two different lithological assemblages, which are coeval and grade laterally to each other. One assemblage is a 'carbonate terminal complex' formed by tidal flat and sabkha deposits, which is predominant in the lower Muschelkalk unit. The other assemblage is a lagoon-peritidal (upper) carbonate-marl alternation, predominant in the upper unit. Together, the two sequences suggest a complex platform morphology with a mosaic facies distribution, which evolved from a not very high energy ramp-like profile (transgressive phases, TST) to a lower energy rimmed shelf, ending with tidal/lagoon environments (regressive phases, HST). Facies associations, however, suggest somewhat deeper depositional settings for the upper than lower Muschelkalk unit. Here we compare the two carbonate units in the study areas with those described in the literature from other Triassic basins of Eastern Iberia and the SW Germanic Basin, all forming part of the Peri-Tethys area of the Tethyan Realm.

1. Introduction

The break-up of Pangea and expansion of the Tethys Ocean to the west began during the Late Permian–Early Triassic (Ziegler, 1982, 1988). As a result of this extensional regime, several sedimentary basins formed in the Iberian Plate (Iberia). During an initial rifting stage, these basins recorded thick detrital successions of non-marine environments (Sakmarian-Anisian *p.p.*). Subsequently, the Tethys waters episodically flooded the eastern part of Iberia during the Middle and Late Triassic (Sopeña et al., 1988; Arche and López-Gómez, 1996; López-Gómez et al., 2002). This occurred in transgressive–regressive cycles, as recorded by a succession of carbonate, detrital-evaporite, and carbonate-evaporite units. The carbonate units correspond to the lower Muschelkalk (Anisian), the upper Muschelkalk (Ladinian), and the Imón Fm and its equivalents (Norian–Rhaetian) (López-Gómez et al., 1998). The detrital-evaporite units correspond to the Röt (Anisian), middle Muschelkalk (Anisian), and Keuper (Carnian–Norian). And finally, the carbonate-evaporite unit corresponds to the Lécera Fm (Anhydrite Zone; Rhaetian–Hettangian) (Ortí et al., 2017).

In the southeastern sector of the Triassic Iberian basin, which is currently part of the eastern Iberian Range (Fig. 1), the stratigraphic record of the transgressive–regressive cycles of the Middle–Upper Triassic has been interpreted in different ways, mainly due to the structural complexity of the sector. During the 60s of the last century, some authors identified in the central (Hinkelbein, 1969) and southeastern (Rambaud, 1962) sectors of the Iberian Range (Albarracín and València areas, respectively), the three stratigraphic Muschelkalk units earlier recognized by Virgili (1958) in the Catalan Coastal Ranges, i.e., lower

* Corresponding author at: Departamento de Estratigrafía y Paleontología, Facultad de Ciencias, Avda. Fuentenueva, 18071 Granada, Spain.
E-mail addresses: aperezl@ugr.es (A. Pérez-López), conbb2@gmail.com (C. Benedicto), f.orti@ub.edu (F. Ortí).

https://doi.org/10.1016/j.sedgeo.2021.105904
0037-0738/

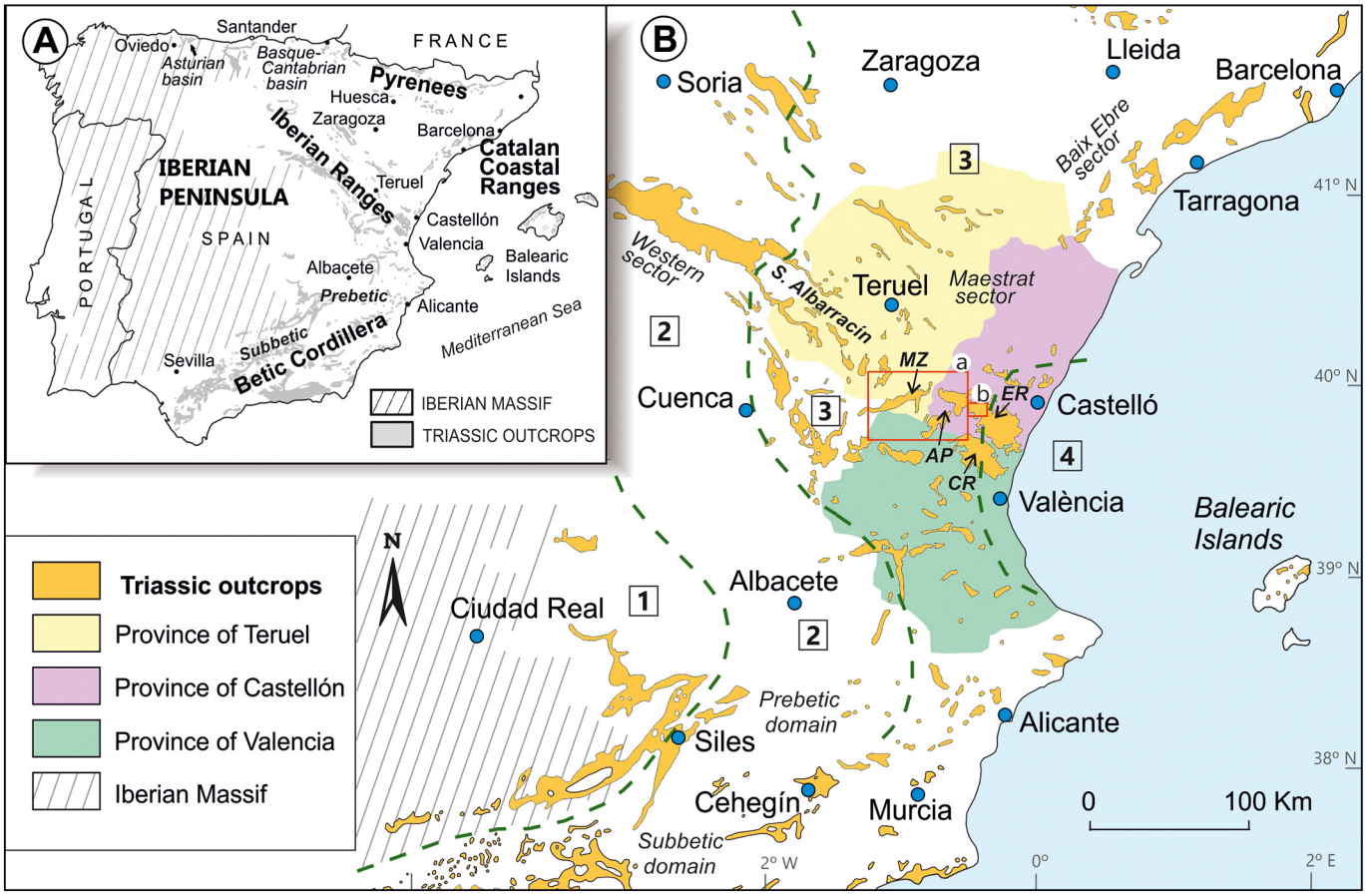

Fig. 1. Triassic outcrops in Eastern Iberia. (A) Distribution of the Alpine ranges in the Iberian Peninsula and the main Triassic basins. (B) Location map of Triassic outcrops in the central and eastern part of the Iberian Range and eastern Prebetic domain and surrounding basins. Green lines mark the boundary between the different paleogeographic types of Triassic according to López-Gómez et al. (1998): (1) Hesperian Triassic; (2) Iberian Triassic; (3) Mediterranean Triassic, (4) Levantine–Balearic Triassic. The study area is indicated with a red rectangle (a). In the small rectangle (b), one of the studied sections is included (Fig. 2). Symbols: AP: Alt Palància area; MZ: Manzanera area; CR: Calderona Ridge; ER: Espina–Espadà Ridge. (For interpretation of the references to color in this figure legend, the reader is referred to the web version of this article.)

Muschelkalk carbonate unit (M1; Anisian), middle Muschelkalk detrital-evaporite unit (M2; Anisian), and upper Muschelkalk carbonate unit (M3; Ladinian). This succession was named 'Mediterranean Triassic' by Virgili et al. (1977) and Sopeña et al. (1983). Subsequently, López-Gómez et al. (1998) defined in the easternmost sector (coastal area) of the València and Castelló provinces and on Menorca Island, the 'Levantine–Balearic Triassic', which was characterized by the presence of a single carbonate Muschelkalk unit of Anisian–Ladinian age (Fig. 1). Recently, Escudero-Mozo et al. (2015) expanded the Levantine sector of this Levantine–Balearic Triassic significantly to the north and west, and also re-assigned all the carbonate Muschelkalk units cropping out in this enlarged sector to the upper Muschelkalk unit of late Anisian–Ladinian age. However, Ortí et al. (2020) recently documented the presence of the Mediterranean Triassic in the Alt Palància area (Castelló province) and adjacent Triassic outcrops to the north and east. These new observations suggest keeping the original boundary line of López-Gómez et al. (1998) to separate the Mediterranean and Levantine–Balearic Triassics in the easternmost sector of the Iberian basin.

The carbonate rocks of the lower and upper Muschelkalk units of the Mediterranean Triassic show clear characteristics of an epicontinental platform (López-Gómez et al., 1998). The complexity of this type of platform has been highlighted in the Betic basin (S and SE of Iberia) by Pérez-López et al. (2011). In these fault-controlled platforms, detail variations in the successions along with their facies similarities make it difficult to distinguish formal members within the stratigraphic formations. This is because the predominant coastal and shallow-marine sediments of these platforms are found irregularly scattered across a complex paleogeography comprised of tidal flats, lagoons and restricted inland seas.

The main aim of this study is to further our understanding of the stratigraphy, sedimentology and paleogeography of carbonate sedimentation during the Middle Triassic in the SE sector of the Iberian basin, as interpretations of the carbonate Muschelkalk units in this region remain controversial. Our study focuses on two areas of the SE Iberian Range, i.e. the Alt Palància area (Castelló province) and the large Manzanera outcrop (Teruel province), with local observations in the adjacent Espina–Espadà Ridge (Fig. 2). In the Alt Palància area, Ortí et al. (2020) have recently conducted a general study (cartography, stratigraphy, palynological dating, sulfate isotopy) of the Middle–Upper Triassic successions. In the present paper, all the observations described for the Manzanera area are new. Our results are compared with data obtained from Muschelkalk carbonate successions in other sectors of the Iberian basin and in the Catalan and Betic basins, all forming part of the westernmost region of the Tethyan Realm. Finally, these data are also compared with the Muschelkalk of the SW Triassic Germanic Basin.

2. Geological setting

The stratigraphic units present in the Triassic outcrops of the two study areas were initially described in the 1:50,000 scale geological maps of Camarena de la Sierra, 613 (IGME, 1978), Manzanera, 614 (IGME, 1974a), Alpuente, 638 (IGME, 1975), Jérica, 639 (IGME, 1977), and Segorbe, 640 (IGME, 1974b) carried out by the Spanish National Program of geological cartography (MAGNA) during the 1970s

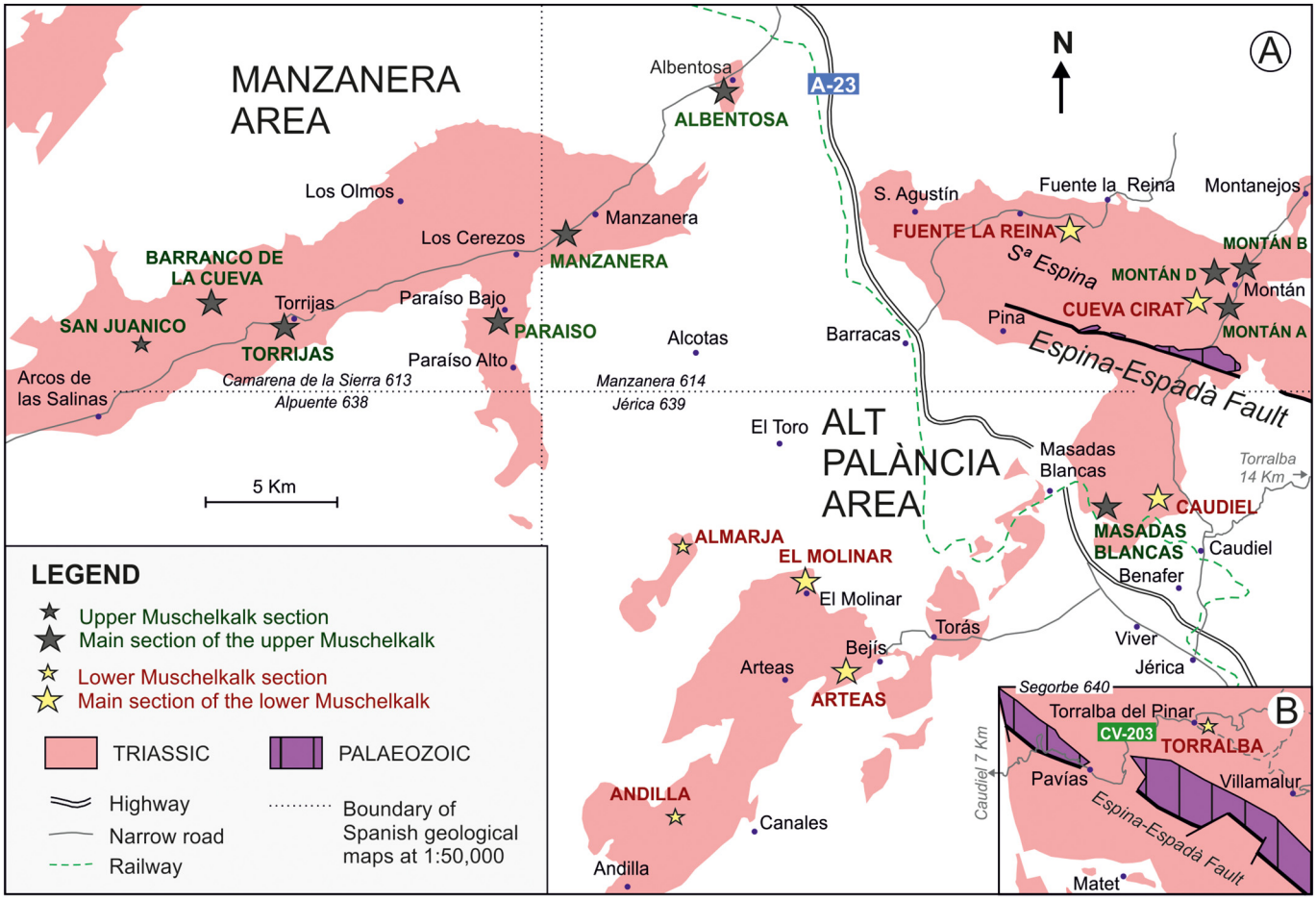

Fig. 2. (A) Location map of the main stratigraphic sections in the study areas (Alt Palància and Manzanera). Representative sections: yellow stars (lower Muschelkalk unit) and dark gray stars (upper Muschelkalk unit). Other sections cited in the text: smaller stars. Geology based on the Spanish Geological Maps (1:50,000 scale) of Manzanera, Segorbe, Alpuente, Jérica and Camarena de la Sierra (respectively, in IGME, 1974a, 1974b, 1975, 1977 and 1978). (B) Location scheme at the same scale of the Torralba del Pinar section to the E of Caudiel village in the Segorbe Map (640) (small rectangle b in Fig. 1). (For interpretation of the references to color in this figure legend, the reader is referred to the web version of this article.)

(Fig. 2). In the Triassic outcrops of these areas, carbonate Muschelkalk units are often found tectonically disrupted and mixed with plastic masses of the middle Muschelkalk and Keuper evaporites. This complex structure precludes any easy identification of the two carbonate Muschelkalk units or finding sections where their stratigraphic record is complete.

In the Alt Palància study area, a major fault is the NW–SE trending Espina–Espadà fault, which acted as an extensional element during the Mesozoic and was lately inverted during Alpine compression allowing for the final outcrop of Paleozoic materials (Fig. 2) (Ortí et al., 2020). In the Manzanera area, several features such as the linear geometry of the Triassic outcrop, its antiform structure, and several thrust sheets of Muschelkalk carbonates in the nucleus of this diapiric structure, suggest the existence of a major basement WNW–ESE fault, although there are only scarce Buntsandstein outcrops and no exposed Paleozoic materials (IGME, 1974a) (Fig. 2).

In these two study areas, different names of formations and members (Fig. 3) have been used for the Middle–Upper Triassic units (Castillo, 1980; López-Gómez and Arche, 1992a; Garay Martín, 2001, 2005; Escudero-Mozo et al., 2015; Ortí et al., 2020; among others). For the Muschelkalk units, the classic terms of lower (M1), middle (M2) and upper Muschelkalk (M3) employed by Ortí et al. (2020) for the Alt Palància are used here. These lower and upper Muschelkalk units correspond to the Landete Fm and Cañete Fm, respectively, of López-Gómez and Arche (1992a), which are the most commonly used terms for the carbonate Muschelkalk units of the central-eastern sectors of the Triassic Iberian basin.

3. Materials and methods

This work is mainly based on stratigraphic, petrographic and sedimentologic studies of selected sections of the Alt Palància and Manzanera Triassic areas (Fig. 2). The sections were logged in detail using a Jacob's staff when necessary, and analyzed by standard sedimentary and paleontologic field methods. To fully characterize the lithofacies of sections, samples were collected for macroscopic observation on polished slabs and microfacies were examined by thin-section observation using a petrographic microscope. The study of carbonate rocks follows the classification of Dunham (1962) with modifications by Embry and Klovan (1971). Alizarin Red S was used to distinguish dolomite from calcite.

For the Alt Palància area, we used the stratigraphic, isotope, and paleontologic data provided by Ortí et al. (2020). To distinguish between the two carbonate Muschelkalk units in this structurally complex area, a palynologic study of all the Middle–Upper Triassic units and an isotope study of gypsum samples in the clayey–gypsiferous units bounding the carbonate ones were needed. According to the palynologic study, Ortí et al. (2020) distinguished between Anisian units (Röt, lower Muschelkalk) and Ladinian units (upper Muschelkalk). The isotope study results were used by Ortí et al. (2020) to differentiate between the middle Muschelkalk and Keuper units, despite the marked similarity of the two evaporite facies. For the present study, all the carbonate Muschelkalk sections in Ortí et al. (2020) were revised, and six of them were selected for detailed lithologic sampling and a petrographic–sedimentologic study.

In the present study of the Manzanera area, a complete stratigraphic analysis was only possible in the upper Muschelkalk unit. Moreover, this

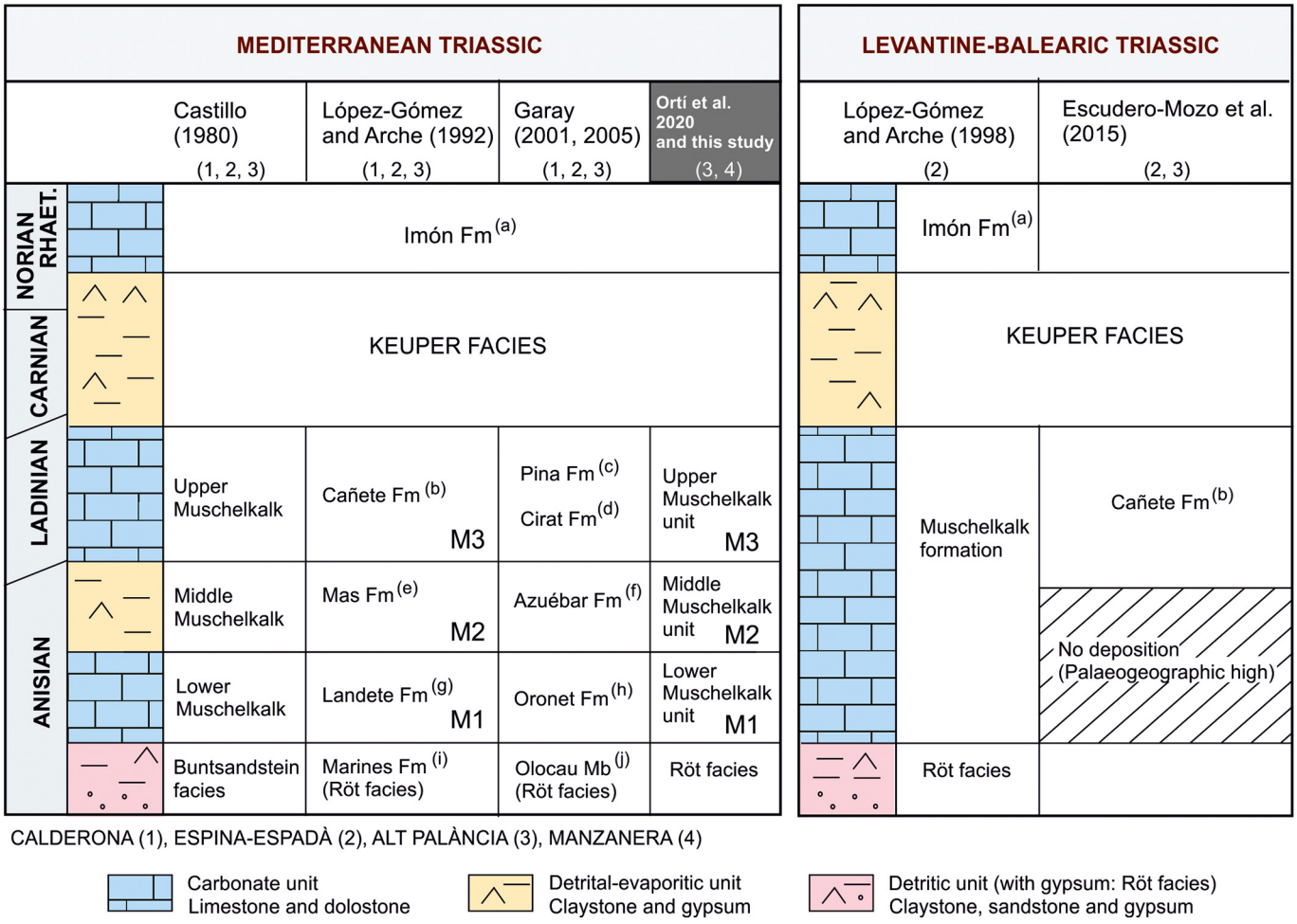

Fig. 3. Stratigraphic framework of the Middle–Upper Triassic successions of the Mediterranean Triassic (areas of Calderona Ridge, Espina–Espadà Ridge, and Alt Palància) and Levantine–Balearic Triassic (compiled after several authors). The formations are: (a) Imón Dolostone Fm; (b) Cañete Dolostone and Limestone Fm; (c) Pina de Montalgrao Dolomitic Limestones Fm; (d) Cirat Dolostone Fm; (e) Mas Clay, Marl and Gypsum Fm; (f) Azuébar sandy Marls Fm; (g) Landete Dolostone Fm; (h) Oronet Dolostones Fm; (i) Marines Clay, Silt, and Marl Fm; (j) Olocau variegated Mb of the Serra Lutites and Sandstones Formation.

unit has been dated by ammonoids in the Paraíso section (López-Gómez et al., 1998; Goy, 1995). For the present purposes, we revised this section in detail and also used it as reference for stratigraphic correlation with five new sections of the upper Muschelkalk unit. However, because of the structural complexity of the outcrop, correlation was difficult for some sections and it was also necessary to identify through isotope analysis the clayey–gypsiferous units (M2 and Keuper) bounding the carbonate Muschelkalk units, especially along the diapiric axis of the outcrop.

Accordingly, this isotope study of Middle–Upper Triassic gypsum samples was carried out in the Manzanera outcrop. All the samples were identified as secondary gypsum, i.e. gypsum derived from hydration near the surface of anhydrite rocks in the subsurface. Results (12 samples) were compared with literature data available for the middle Muschelkalk and Keuper facies in several Triassic basins of Iberia (Utrilla et al., 1992; Alonso-Azcárate et al., 2006; Iríbar and Ábalos, 2011; Ortí et al., 2014), and in particular in the Catalan basin (Ortí et al., 2018) and Alt Palància sector of the Iberian basin (Ortí et al., 2020).

For this analysis ($\delta^{34}S_{V\text{-}CDT}$ and $\delta^{18}O_{V\text{-}SMOW}$, in ‰), each gypsum sample was dissolved in distilled water, acidified to pH 3 by adding HCl and then reprecipitated as barium sulfate by means of a solution of $BaCl_2$. Sulfur and oxygen isotope compositions were analyzed by the *on-line* method. $\delta^{34}S_{V\text{-}CDT}$ was determined with a Carlo Erba 1108 Elemental Analyzer and $\delta^{18}O_{V\text{-}SMOW}$ with a TC-EA unit, both coupled to an IRMS ThermoFisher Delta Plus XP at the Stable Isotope Laboratory of the CCiTUB (Universitat de Barcelona). The $\delta^{34}S$ and $\delta^{18}O$ values obtained are reported in ‰ relative to the Vienna Canyon Diablo Troilite (V-CDT) standard for sulfur and to the Vienna SMOW (V-SMOW) standard for oxygen.

4. Lithostratigraphy

For the Alt Palància area, the six stratigraphic sections described in Ortí et al. (2020) and revised and completed here were: Arteas, Molinar (El Molinar), Masadas Blancas, Caudiel, Cueva Cirat and Montán. In addition, a new section (Torralba del Pinar, in the Espadà Ridge) was examined in detail (Fig. 2B). Apart from the Paraíso section, the five new sections studied in the Manzanera area were: San Juanico, Barranco de la Cueva, Torrijas, Manzanera, and Albentosa (Figs. 4 to 8).

The lower Muschelkalk sections of Molinar and Cueva Cirat in the Alt Palància area were assigned to the upper Muschelkalk unit (Cañete Fm)

Fig. 4. Representative stratigraphic sections (Arteas, Molinar, Caudiel) of the lower Muschelkalk unit (M1) in the Alt Palància area. Section location in Fig. 2A. Capital letters represent main facies. U.T.M. coordinates (ED50; zone 30 in all sections) of the base of the sections: Arteas: X: 694889, Y: 4420113; Molinar: X: 693585, Y: 4423892; Caudiel: X: 705115, Y: 4428185.

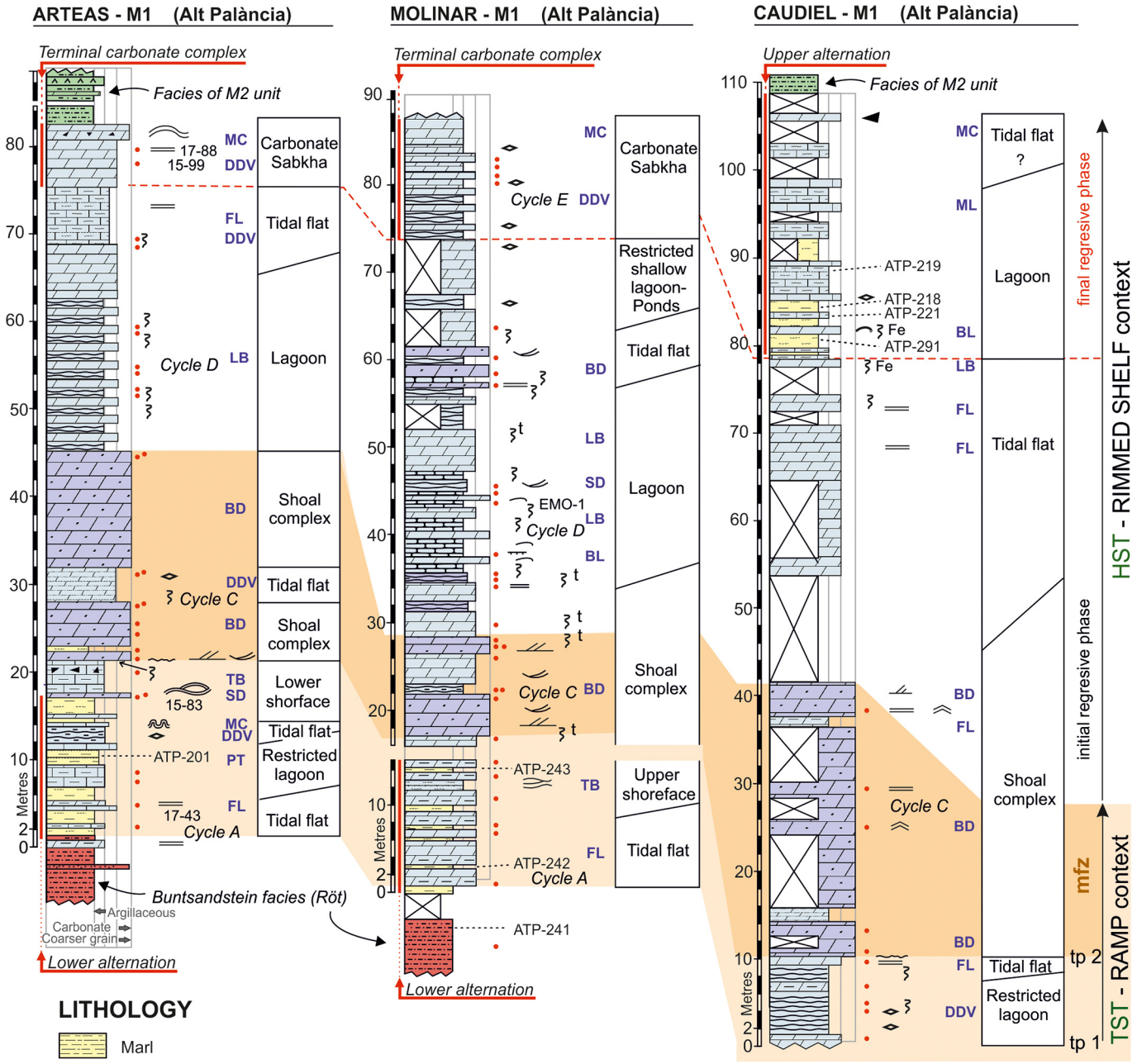

LITHOLOGY

- Marl
- Undulated thin bedded marly carbonate and marl
- Dolosparite (Calcarenite)
- Dolomite
- Limestone
- Ochre carniolar carbonate
- Marly limestone/dolomite
- Wave-bedded limestone
- Paper thin-bedded marly limestone
- Bioturbated nodular limestone
- Red to variegate lutite
- Sandstone
- Gypsum

SEDIMENTARY STRUCTURES AND FOSSILS

- Planar cross-lamination
- Cross-lamination (low angle)
- Undulated bedding
- Trough cross-bedding
- Parallel lamination
- Wave ripples
- Slump
- Hummocky cross-bedding
- Breccia
- Gutter cast
- Burrow (on top)
- Boring
- Stromatolite
- Stromatolytic dome
- Bioclastic grains
- Bivalve mold
- Crinoid
- Evaporite mold/cast
- Erosional surface
- Hardground
- Fe Iron oxide mineralization
- Rock sample
- EMO-1 Carbonate sample for crinoids
- S-# Gypsum sample for S isotope
- ATP-# Lutite/marl palynological sample (Ortí et al., 2020)

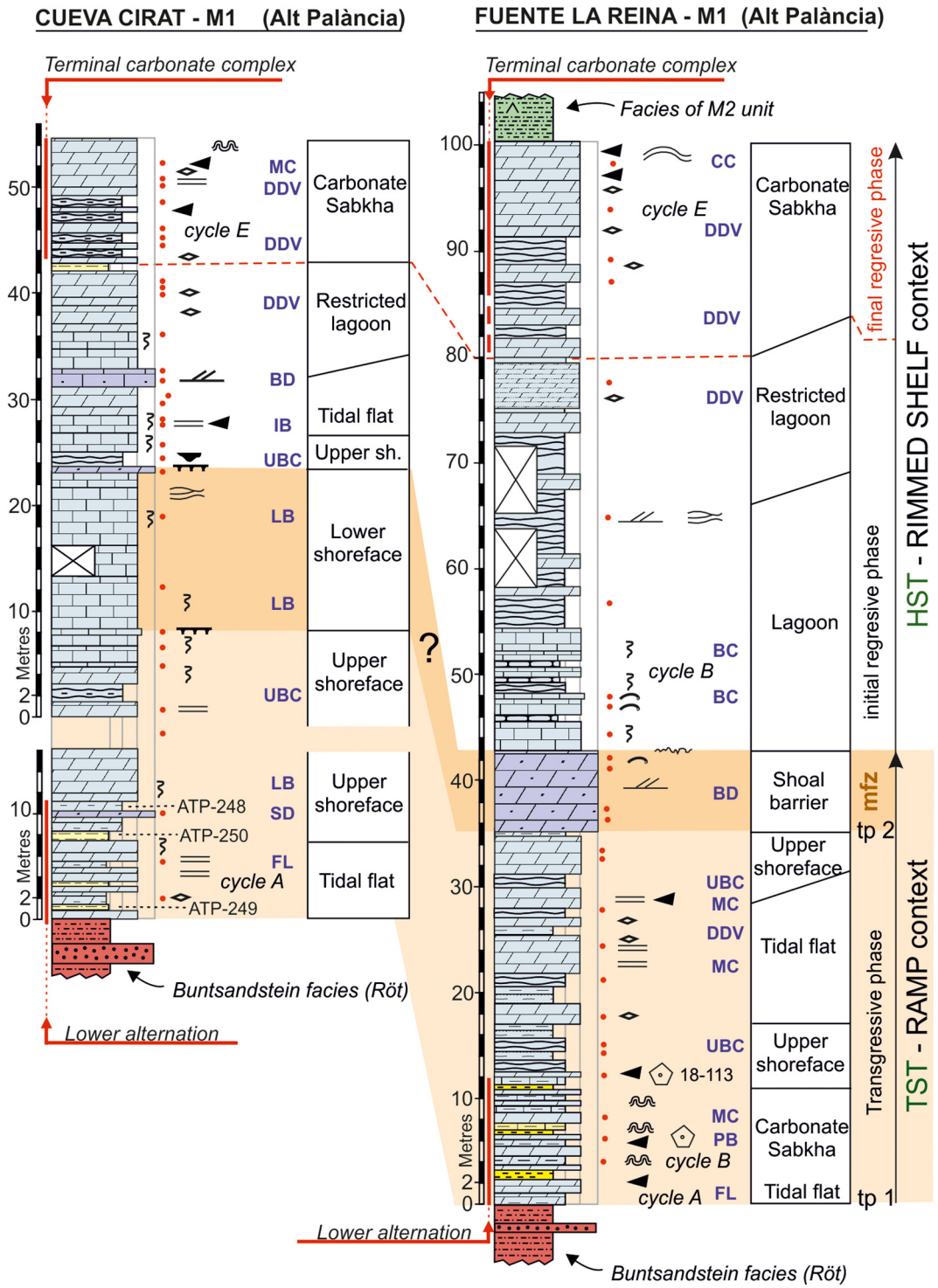

Fig. 5. Representative stratigraphic sections (Cueva Cirat, Fuente la Reina) of the lower Muschelkalk unit (M1) in the Alt Palància area. Section location in Fig. 2A and legend in Fig. 4. Capital letters represent main facies. U.T.M. coordinates (ED50; zone 30 in all sections) of the base of the sections: Cueva Cirat: X: 707676, Y: 4433841; Fuente la Reina: X: 704657, Y: 4435505.

in Escudero-Mozo et al. (2015) and Escudero-Mozo et al. (2015). In the present study, these sections are attributed to the lower Muschelkalk unit following Ortí et al. (2020). Also, the Torralba del Pinar section in the same area, which was initially studied and assigned to the lower Muschelkalk unit by Garay Martín (2001, 2005), is here attributed to the lower Muschelkalk unit (Fig. 3).

In terms of lithology, the two carbonate Muschelkalk units can be divided into the three sub-units previously identified by Ortí et al. (2020) in the Alt Palància area, i.e. lower carbonate-marl alternation, middle carbonate sub-unit, and upper carbonate-marl alternation. In some sections, however, the upper carbonate-marl alternation is replaced with a 'terminal carbonate complex' (new term used in the present paper). The possible equivalences of these sub-units with the stratigraphic members used by other authors are shown in Supplementary data A and B for the lower and the upper Muschelkalk units, respectively.

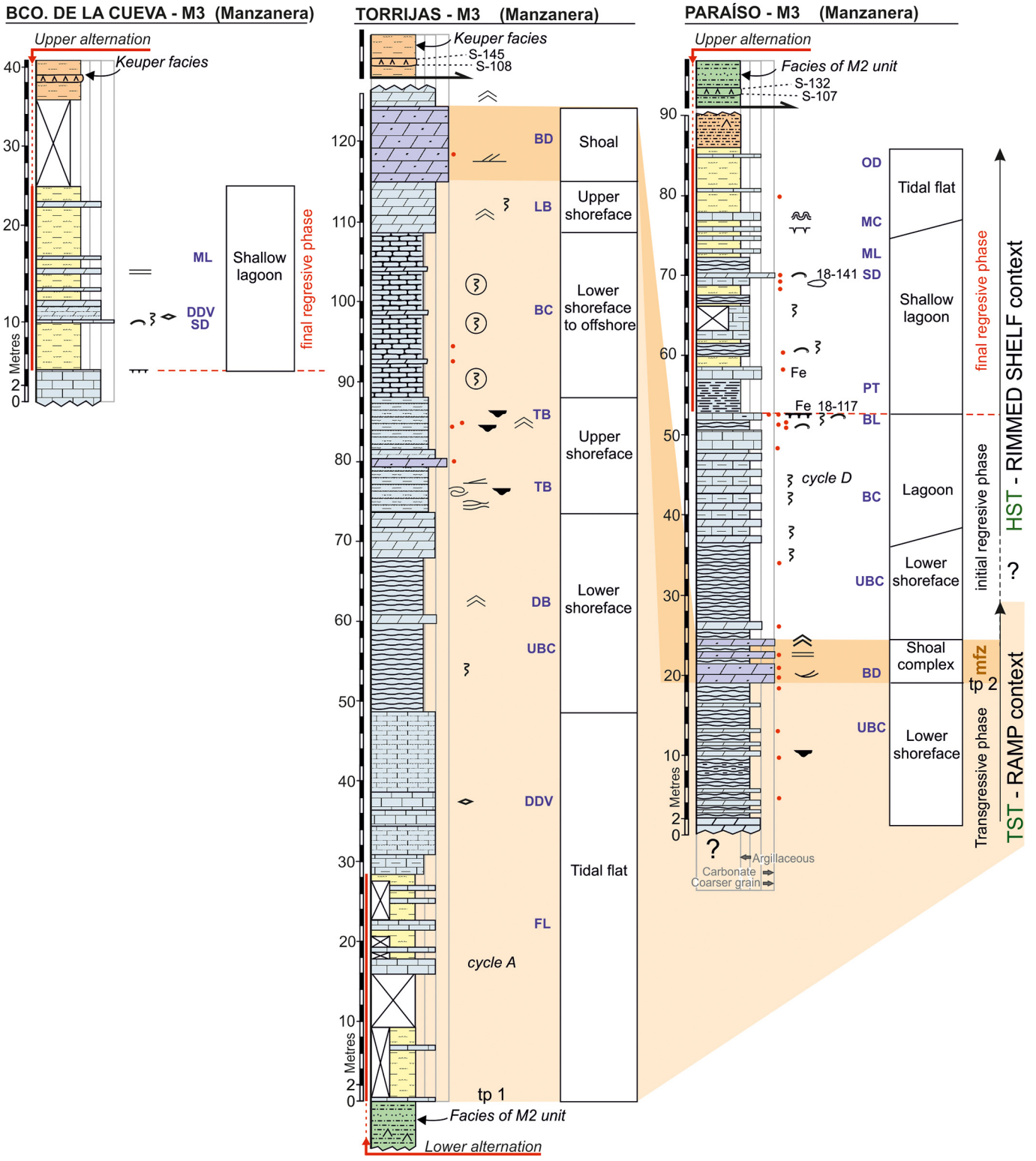

Fig. 6. Representative stratigraphic sections (Barranco de la Cueva, Torrijas, Paraíso) of the upper Muschelkalk unit (M3) in the Manzanera area. Section location in Fig. 2A and legend in Fig. 4. Capital letters represent main facies. U.T.M. coordinates (ED50; zone 30 in all sections) of the base of the sections: Bco. de la Cueva: X: 0670623, Y: 4434189; Torrijas: X: 0673844, Y: 4431836; Paraíso: X: 0681973, Y: 4433377.

5. Biostratigraphy

Given the scarcity of macrofossils, especially ammonoids, dating and correlating the two carbonate Muschelkalk units of the study areas is not an easy task. As stated above, a first attempt to distinguish and date these units through palynology was made in the Alt Palància area by Ortí et al. (2020). Some observations by these authors can be highlighted: (a) the Anisian age of all samples from the lower and middle Muschelkalk unit; (b) the absence of Anisian assemblages in all samples belonging to the lower carbonate-marl alternation of the upper Muschelkalk unit; and (c) the Ladinian age of assemblages detected throughout the whole upper Muschelkalk unit.

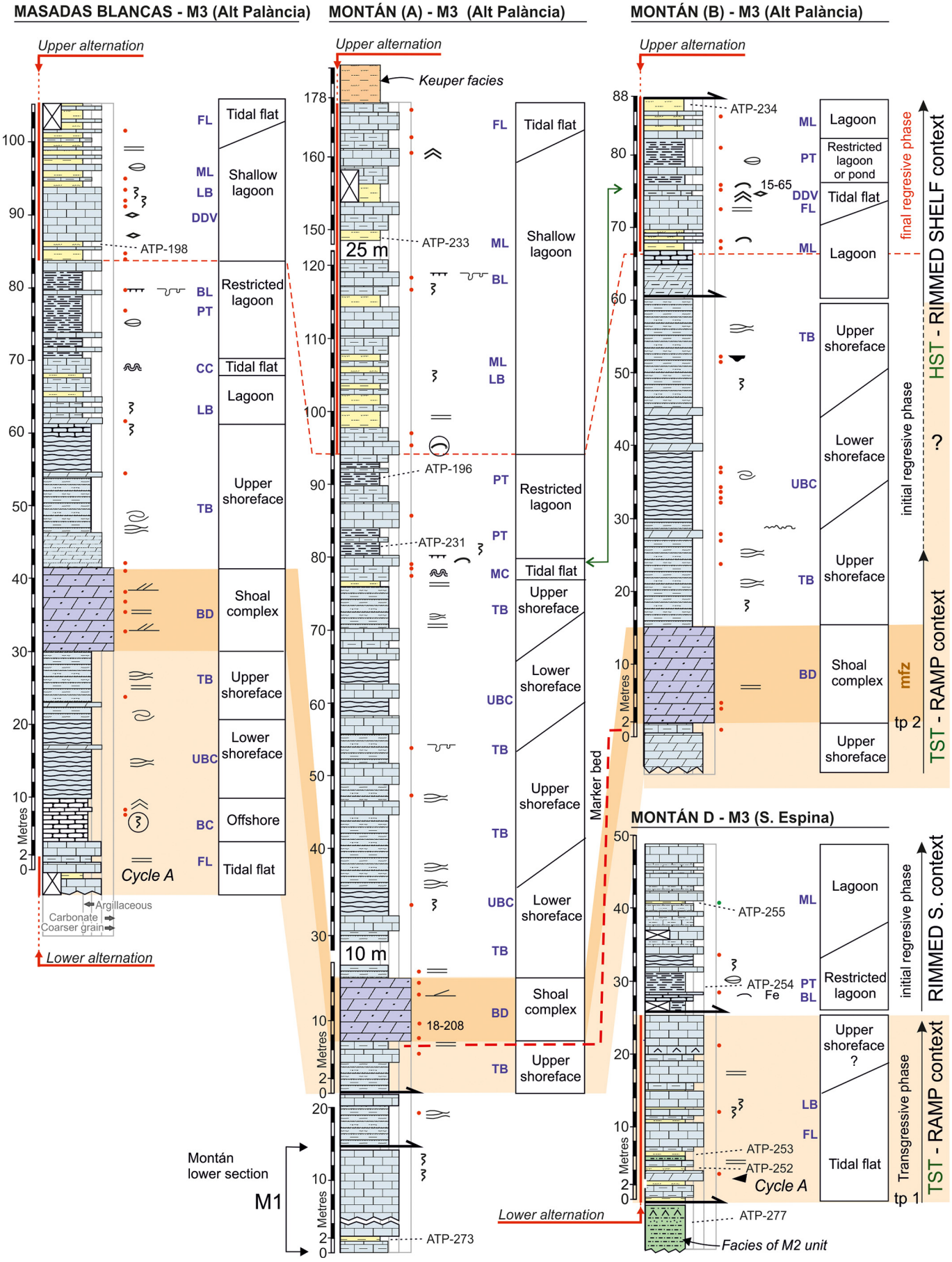
MASADAS BLANCAS - M3 (Alt Palància)
MONTÁN (A) - M3 (Alt Palància)
MONTÁN (B) - M3 (Alt Palància)
MONTÁN D - M3 (S. Espina)
Upper alternation
Lower alternation
Keuper facies
ATP-198
ATP-233
ATP-196
ATP-231
18-208
ATP-234
ATP-255
ATP-254
ATP-253
ATP-252
ATP-277
ATP-273
15-65
25 m
10 m
Metres
Cycle A
Argillaceous
Carbonate
Coarser grain
Tidal flat
Shallow lagoon
Restricted lagoon
Lagoon
Upper shoreface
Lower shoreface
Shoal complex
Offshore
Restricted lagoon or pond
Marker bed
Montán lower section
M1
Facies of M2 unit
final regresive phase
initial regresive phase
Transgressive phase
HST - RIMMED SHELF context
TST - RAMP context
RIMMED S. context
mfz
tp 1
tp 2
?

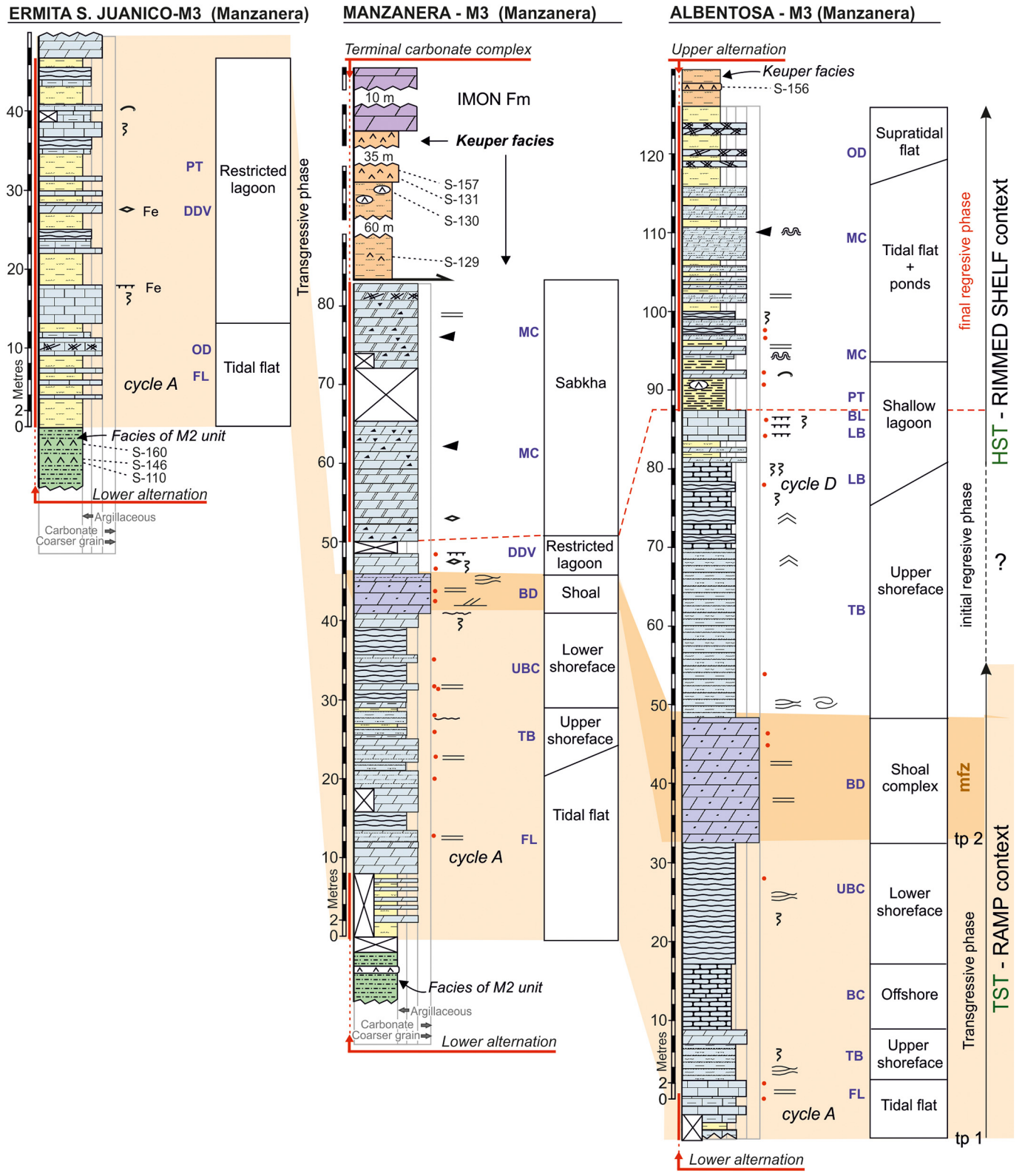

Fig. 8. Representative stratigraphic sections (Ermita de San Juanico, Manzanera, Albentosa) of the upper Muschelkalk unit (M3) in the Manzanera area. Section location in Fig. 2A and legend in Fig. 4. Capital letters represent main facies. U.T.M. coordinates (ED50; zone 30 in all sections) of the base of the sections: Ermita S. Juanico: X: 0668929, Y: 4431200; Manzanera: X: 0684399, Y: 4435302; Albentosa: X: 06899870, Y: 4441358.

Fig. 7. Representative stratigraphic sections (Masadas Blancas, Montán) of the upper Muschelkalk unit (M3) in the Alt Palància area. In the composite Montán section, portions A, B, and D are the same as in Ortí et al. (2020) (portion C of the Keuper facies was excluded from the present study). Portion (A) of this section shows a thickness of almost 90 m in the upper carbonate-marl alternation (54 m were measured by Garay Martín, 2001, p. 114, based on the identification of a local fault). Section location in Fig. 2A and legend in Fig. 4. Capital letters represent main facies. U.T.M. coordinates (ED50; zone 30 in all sections) of the base of the sections: Masadas Blancas: X: 703466, Y: 4426961; Montán (A): X: 708404, Y: 4433745; Montán (B): X: 709378, Y: 4435957; Montán (D): X: 708245, Y: 4434773.

Table 1
Age assignments of the different sections.

Section	Age assignment	Stratigraphic unit (subunit)	Unit	Data (references)
Alt Palancia area				
Montán A-D	Ladinian	Upper Muschelkalk (upper alternation)	M3	Palynological analysis (Ortí et al., 2020).
Masadas Blancas	Ladinian	Upper Muschelkalk (upper alternation)	M3	Palynological analysis (Ortí et al., 2020) and stratigraphic correlation.
Arteas	Anisian	Lower Muschelkalk (lower alternation)	M3	Palynological analysis (Ortí et al., 2020).
Molinar	Anisian	Lower Muschelkalk (lower alternation)	M1	Palynological analysis (Ortí et al., 2020) and Anisian Crinoide.
Almarja	Anisian	Lower Muschelkalk (lower alternation)	M1	Palynological analysis (Ortí et al., 2020).
Caudiel	Anisian	Lower Muschelkalk (upper alternation)	M1	Palynological analysis (Ortí et al., 2020).
Montán (M1, Fig. 7A)	Anisian	Lower Muschelkalk (lower alternation)	M1	Palynological analysis (Ortí et al., 2020).
Cueva Cirat	Anisian	Lower Muschelkalk	M1	Palynological analysis (Ortí et al., 2020), foraminifera (Escudero-Mozo et al., 2012) and stratigraphic correlation.
Fuente la Reina	Anisian	Lower Muschelkalk (lower alternation)	M1	Palynological analysis (Ortí et al., 2020) and stratigraphic correlation.
Manzanera area				
Barranco de la Cueva	Ladinian	Upper Muschelkalk (upper alternation)	M3	Stratigraphic correlation.
Torrijas	Ladinian	Upper Muschelkalk (gypsum in the overlying Keuper unit)	M3	Stratigraphic correlation and S isotope analysis.
Paraíso	Ladinian	Upper Muschelkalk	M3	Ammonoids (Goy, 1995; Escudero-Mozo et al., 2015)
Ermita San Juanico	Ladinian	Upper Muschelkalk (lower alternation) (gypsum in the underlying middle Muschelkalk unit)	M3	Stratigraphic correlation and S isotope analysis.
Manzanera	Ladinian	Upper Muschelkalk (gypsum in the overlying Keuper unit)	M3	Stratigraphic correlation and S isotope analysis.
Albentosa	Ladinian	Upper Muschelkalk (gypsum in the overlying Keuper unit)	M3	Stratigraphic correlation and S isotope analysis.

No Anisian ammonoids have been identified in the lower Muschelkalk unit (Landete Fm) in the Iberian Ranges, except in the Molinar section of the study area (Goy, 1995). This section was assigned to the Landete Fm (lower Muschelkalk unit) by López-Gómez et al. (1998), and the same designation was assumed in Ortí et al. (2020; see Appendix I, section S8). These observations are in agreement with the present work (Table 1), in which the Molinar section is also assigned to the lower Muschelkalk unit based on the presence of the Anisian crinoid, *Holocrinus dubius* (Goldfuss), in the middle part of the section (A.E. Götz personal communication) (Fig.4). For the upper Muschelkalk unit, Ladinian ammonoids have not been described in the stratigraphic sections of the Alt Palància area.

As mentioned earlier, no Ladinian ammonoids were identified in the Manzanera outcrop except in the Paraíso section (Goy, 1995; Escudero-Mozo, 2015; Escudero-Mozo et al., 2015) allowing its assignment to the Cañete Fm (upper Muschelkalk unit).

6. Sulfate isotopy

The stratigraphic position of the studied samples in the Manzanera outcrop is shown in Figs. 4 to 8, and the corresponding isotope results are shown in Table 2. The gypsum samples assigned according to stratigraphic criteria to the middle Muschelkalk unit (5 samples) yielded $\delta^{34}S$ values of 15.8‰ to 17.0‰ with a mean of 16.4‰, and $\delta^{18}O$ values of 13.0‰ to 17.8‰ with a mean of 15.6‰. The gypsum samples that according to stratigraphic criteria should belong to the Keuper unit (7 samples) yielded $\delta^{34}S$ values of 13.8‰ to 15.7‰ with a mean of 14.7‰, and $\delta^{18}O$ values of 12.3‰ to 17.9‰ with a mean of 14.8‰.

Of most interest was the assemblage of $\delta^{34}S$ values, which according to the data of Ortí et al. (2018, 2020) assign the gypsum samples either to the middle Muschelkalk or Keuper unit. In the Alt Palància outcrops, $\delta^{34}S$ values for the middle Muschelkalk unit were 15.6 to 17.8‰ with a mean of 16.4‰ (14 samples), and of the Keuper unit were 14.0 and 15.5 ‰ with a mean of 14.4‰ (15 samples). In the Triassic Catalan basin, $\delta^{34}S$ values for the middle Muschelkalk unit were 16.5 to 18.7‰ with a mean of 17.8‰ (38 samples), and of the Keuper units were 14.2 to 15.4‰ with a mean of 15.0 ‰ (10 samples).

The $\delta^{34}S$ values obtained here for the middle Muschelkalk and Keuper units of the Manzanera outcrop are consistent with those provided above for the corresponding units of the Catalan basin and the Alt Palància sector of the Iberian basin (Table 2). In the Manzanera outcrop, as stated above, the lowest value found in the middle Muschelkalk unit was 15.8‰ and the highest $\delta^{34}S$ value found in the Keuper unit was 15.7‰, this pair of values defining the $\delta^{34}S$ boundary for the two units of this outcrop. Thus, good correspondence was found between the $\delta^{34}S$ value of each sample and its expected stratigraphic unit (Figs. 4 to 8). However, an anomalous case was recorded in the Paraíso section, where a clayey–gypsiferous unit characterizing the middle Muschelkalk unit (two gypsum samples with $\delta^{34}S$ values of 16.2 and 17.0‰) overlies the upper marl-carbonate alternation of the upper Muschelkalk unit. A faulted contact (thrust) between the two units is here assumed.

Table 2
Isotope results for the Manzanera area. Projection UTM, datum ED50, Zone 30.

Section	Sample	Gypsum lithofacies	$\delta^{34}S$ (‰)	$\delta^{18}O$ (‰)	Assigned stratigraphic unit	Coordinates (UTM)
Albentosa	156 (YsMz-14)	Nodular	15.0	17.9	Keuper	30T 0690283 4441390
Manzanera	129 (YsMz-16)	Massive	14.0	12.7	Keuper	30T 0684032 4435251
Manzanera	130 (YsMz-17)	White nodular	14.5	14.8	Keuper	30T 0684452 4435086
Manzanera	157 (YsMz-18)	White laminated	15.1	12.3	Keuper	30T 0684525 4434907
Manzanera	131 (YsMz-19)	White massive	14.9	13.0	Keuper	30T 0684530 4434892
Paraíso	132 (YsMz-2)	Dark laminated	17.0	14.4	Middle Muschelkalk	30T 0682186 4432915
Paraíso	107 (YsMz-3)	Pink nodular	16.2	16.5	Middle Muschelkalk	30T 06822184 4432915
Torrijas	108 (YsMz-6)	Nodular	13.8	15.0	Keuper	30T 0673644 4432220
Torrijas	145 (YsMz-7)	Pink laminated	15.7	17.7	Keuper	30T 0673530 4432135
San Juanico	110 (YsMz-29)	Porphyroblastic massive	15.8	13.0	Middle Muschelkalk	30T 0668929 4431200
San Juanico	146 (YsMz-21)	Dark laminated	16.5	16.4	Middle Muschelkalk	30T 668934 4431203
San Juanico	160 (YsMz-22)	Dark laminated	16.4	17.8	Middle Muschelkalk	30T 668902 4431218

7. Facies analysis

Numerous types of carbonate facies exist in the lower and upper Muschelkalk units of the study areas. Most facies are similar for the two units although there are also marked differences depending on the sections, especially at their tops. Most of the Triassic deposits correspond to fine-grained carbonates and are quite homogeneous. From the study of thin sections, it is observed that most of the microfacies consist of mudstones or microsparstones. Despite this, it is possible to define up to fifteen main facies (Figs. 9, 10, 11 and Table 3), which are grouped into seven genetically linked lithofacies associations (FA). These facies associations are assigned to different sedimentary environments of the carbonate platform. According to the depth at which different processes interact with the sea floor (tides, fair weather wave base and storm wave base) these associations are assigned also to foreshore, upper shoreface, lower shoreface and offshore.

7.1. Undulating bedded carbonate (Facies UBC)

This facies is common in the Triassic carbonates of Eastern Iberia. Mainly, it consists of thin bedded (1 to 5 cm thick) dark gray dolostone with undulated surfaces, i.e. this facies features undulated bottoms or tops. Undulations can vary in their dimensions from one bed or one section to another (Fig. 9A). Variable amounts of clay can be found interlayered in the carbonate beds. Although clay is normally scarce, in some sections it is altogether absent between the carbonate thin beds and may show some bioturbation structure.

Microfacies. This is dolomicrosparstone (mudstones). In thin-sections, bioclasts or peloids are very rare. Only microsparite is observed.

Interpretation. The present facies is interpreted based on its microfacies and lithologic features as lower shoreface deposits

Fig. 9. Lithofacies in outcrop. (A) Undulating bedded carbonate (Facies UBC) with undulated surfaces (Masadas Blancas section, Fig. 7). (B) Thin-bedded carbonate and marl (Facies TB) showing low angle cross-stratification (Torrijas section, Fig. 6). (C) Thin-bedded carbonate with gutter casts (red arrow) (Torrijas section, Fig. 6). (D) Brown dolosparite (Facies BD) with trough cross-bedding interpreted as a bioclastic shoal (Arteas section, Fig. 4). (E) Bioturbated nodular carbonate (Facies BC) with bioturbated texture (Torrijas section, Fig. 6). (F) Marly limestone with bioturbation (Facies LB) known as 'fucoides' limestones (Andilla section; location in Fig. 2). (For interpretation of the references to color in this figure legend, the reader is referred to the web version of this article.)

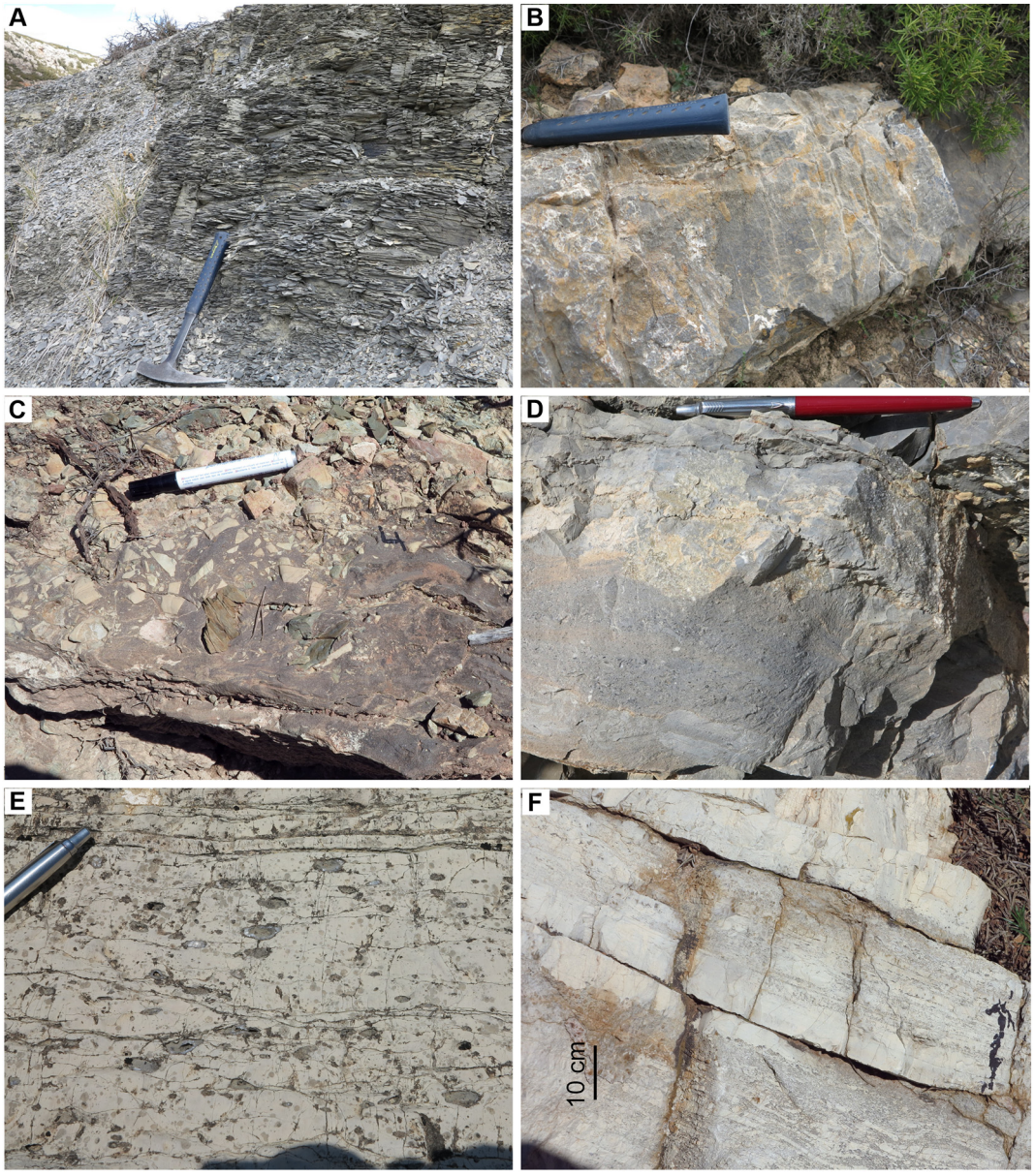

Fig. 10. Lithofacies in outcrops. (A) Paper-thin bedded marly limestone (Facies PT) (Albentosa section, Fig. 8). (B) Bioclastic limestone bearing Balanoglossites (Facies BL) characterized by the ochre ferroan dolomite of burrows (Caudiel section, Fig. 4). (C) Polymictic breccia (Facies PB) with carbonate and lutite clasts and crinoid grains (Fuente la Reina section, Fig. 5). (D) Shell-debris limestone (Facies SD) with amalgamated intervals of mollusk fragments (Torralba section; location in Fig. 2B). (E) Dolostone with evaporite dissolution vugs (Facies DDV) and laminations in the upper part (Arteas section, Fig. 4). (F) Stromatolites and laminites of the microbial carbonate facies (Facies MC) with brecciated levels (Fuente la Reina section, Fig. 5).

(Knaust, 1998; Noack and Schroeder, 2003) formed under shallow water and low energy conditions, and locally with some tempestite bed (Facies SD). The lack of mollusk fossils, scarce bioturbation, as well as the dark sediment color suggest oxygen-depleted conditions.

Undulated forms could be interpreted as seabed molding due to waves. However, similar facies are common in the lower Muschelkalk of Germany (Wellenkalke facies) which are interpreted as marly limestone with a wavy appearance (flaser-bedded limestone) due to bioturbation and subsequent overprint by pressure-solution (e.g., Ricken and Eder, 1991; Zwenger, 1993). Their origin has been debated and although the facies studied by different authors have many similarities, because of the wavy forms of diagenetic origin, their sedimentary origin may vary from one section to another. Diedrich (2009) describes in the Germanic Triassic thin-bedded marly limestones with irregular carbonate waves surfaces which are interpreted as subtidal flat deposits. Pöppelreiter (2002) interpreted similar facies as outer ramp deposits. Noack and Schroeder (2003) consider that this facies corresponds to both inner ramp deposits and middle and outer ramp deposits, depending on the type of microfacies.

7.2. Thin-bedded carbonate and marl (Facies TB)

This carbonate facies consists of bedded limestones or dolostones (3 to 15 cm thick), often bearing thin intercalations of marls (0.5–5 cm thick). Bed surfaces are often slightly undulated, and locally show low-angle cross-stratification (Fig. 9B) or wide erosive channels, which are not very incisive, and intraformational truncation surfaces. Some deformation as small slumps or gutter casts may occur (Fig. 9C). In some sections, this facies grades into the UBC facies.

Microfacies. Common microfacies is dolomicrosparstone, probably mudstone at its origin, in which some bioclasts are recognized (bivalve, peloid).

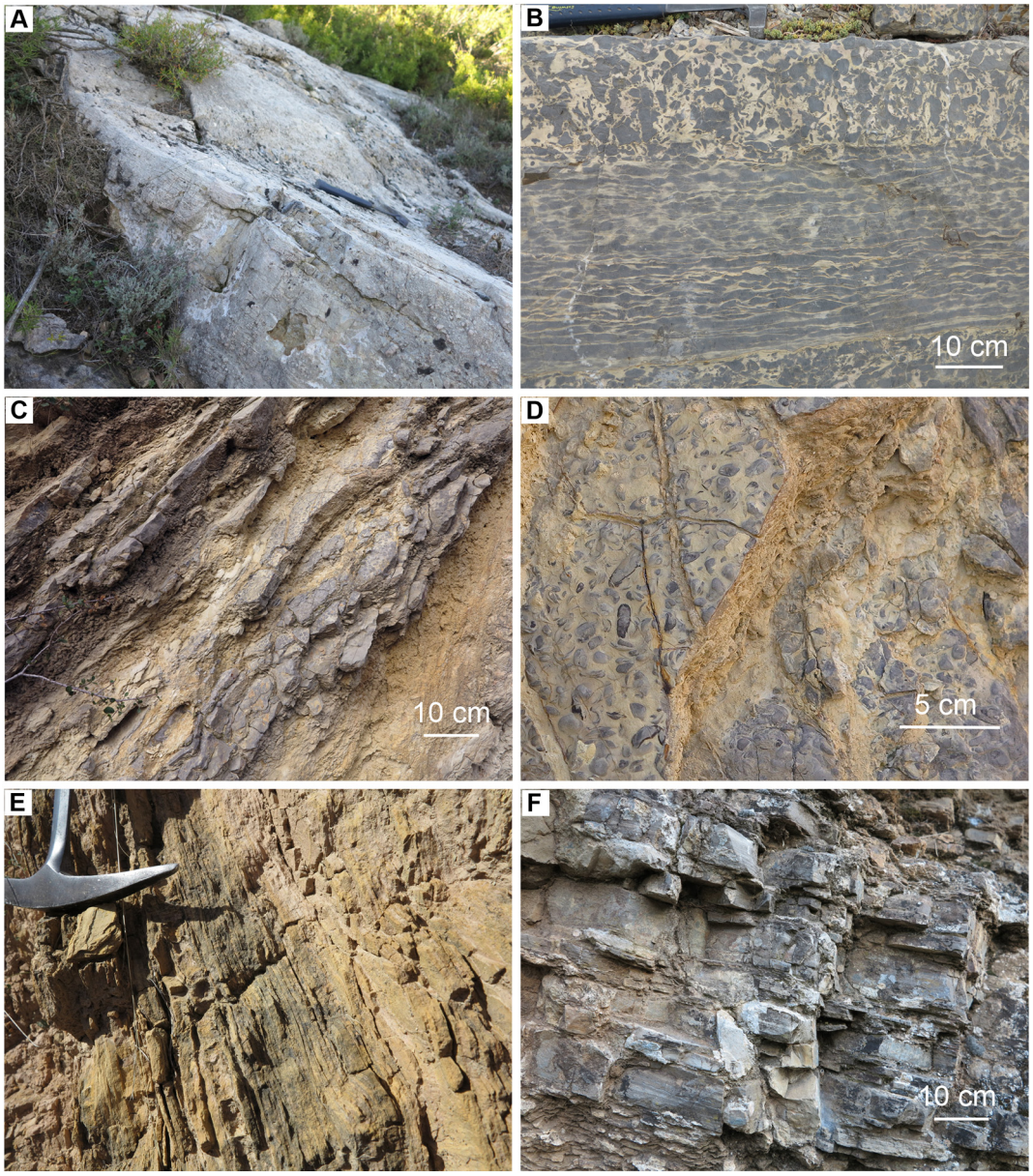

Fig. 11. Lithofacies in outcrop. (A) Stromatolite domes of microbial carbonate (Facies MC) situated at the top of the 'terminal carbonate complex' (Fuente la Reina section, Fig. 5). (B) Intraformational breccia (Facies IB) interpreted as subtidal deposits (Cueva Cirat section, Fig. 5), only appearing in the lower Muschelkalk north of the Espina–Espadà fault. (C) Marl and thin limestone beds with shells (Facies ML) of the upper carbonate-marl alternation (Masadas Blancas section, Fig. 7). (D) Detail of shells (Bakevellia and Pseudocorbula), top surface in facies ML. (E) Ochre dolomite and marl (Facies OD) with algal mats on the top of the upper Muschelkalk succession (Albentosa section, Fig. 8). (F) Fine-laminated carbonate (Facies FL) with depositional thin laminations and algal mats of varying clay contents (Masadas Blancas section, Fig. 7).

Interpretation. Some of the undulated surfaces of this thin-bedded carbonate facies are the result of compaction processes, especially when surfaces are smooth. However, some surfaces are more pronounced and display other sedimentary structures such as cross-stratification, gutter casts or erosive surfaces, which are related to waves or to tidal and storm currents. Similar cross-bedding was described by Duringer and Vecsei (1998), who interpreted it as channel-fill, lateral accretion bedding typical of subtidal deposits. Thus, this facies represents the variation and combination of different currents or hydrodynamic conditions under the influence of waves, tidal currents and storms. All these features are interpreted as shallow ramp deposits (Pérez-Valera and Pérez-López, 2008), mainly of the upper shoreface zone (subtidal zone). Slumps are a common structure in similar facies of the lower Muschelkalk successions of Germany, appearing in fine-grained marly limestones on a slightly inclined carbonate ramp (Knaust, 2000).

7.3. Brown dolostone (Facies BD)

Carbonate beds comprised of brown mesocrystalline dolostone, with a bed thickness between 1 and 15 m, appear in all sections. Commonly this dolostone is massive, although some intervals with parallel lamination, cross- or trough-stratification occur. In some sections, an erosive surface can be identified at the base of these dolostones (Fig. 9D).

Microfacies. It is mainly dolosparstone and generally mesocrystalline, although the size of the crystals may vary. In thin-section, it is possible to distinguish ghosts of ooids or of bioclasts (crinoids, bivalves), mainly crinoids in the lower Muschelkalk unit and ooids in the upper Muschelkalk unit, which could correspond to original grainstones (Fig. 12A, B).

Interpretation. This facies is interpreted as a high-energy deposit based on its sedimentary structures and crystallinity linked to

Table 3
Facies and environmental characteristics of the lower and upper Muschelkalk carbonate units.

Facies	Main features	Microtexture and main components	Depositional environment	M1 unit	M3 unit
1. Facies UBC Undulating bedded carbonate Fig. 9A	Thin bedded dolostone with undulating surfaces.	Dolomicrosparstone. No grains	Lower shoreface	+	++
2. Facies TB Thin-bedded carbonate and marl Fig. 9B	Bedded limestone or dolostone with thin marl bed and undulated surface, with gutter casts, cross-stratification and erosive surface.	Dolomicrosparstone mudstone (?) with rare bivalve or peloid	Upper shoreface	–	++
3. Facies BD Brown dolostone Figs. 9D, 12A, B	Brown dolostone, massive or with cross stratification, erosive surface at the base.	Dolosparstone with ghost of ooids or crinoids	Shoal, barrier Tidal channel	++	++
4. Facies BC Bioturbated nodular carbonate Figs. 9E, 12C	Carbonate with bioturbation texture (pseudobreccia)	Dolosparstone. No grains	Offshore Lower shoreface	–	+
5. Facies LB Marly limestone with bioturbation Fig. 9F	Gray marly limestone beds with scarce to moderate bioturbation	Mudstones to wackestones with mollusks or echinoderms	Subtidal flat Lagoon	++	++
6. Facies PT Paper-thin bedded marly limestone Figs. 10A, 12D	Dark gray marly carbonate or lutite with fine laminated	Mudstones. No grains	Restricted lagoon	+	++
7. Facies BL Bioclastic limestone with Balanoglossites Figs. 10B, 13A	Bioclastic limestone with ochre burrows and bioclast fragments	Wackestone to packstone/rudstone with mollusks and echinoderms	Shallow lagoon Subtidal flat	+	++
8. Facies PB Polymictic breccia Figs. 10C, 13B	Carbonate breccia with carbonate and laminated lutite clasts	Grainstone/rudstone with crinoids	Lag deposits on tidal flat - sabkha	+	–
9. Facies SD Shell-debris limestone Figs. 10D, 13C, D, 14C	Limestones with bioclastic fragments, with sedimentary structures (graded beds, parallel or cross lamination)	Packstone/floatstone Grainstone/rudstone with mollusks, echinoderm, peloids, ooids, quartz grains	Storm deposits (tempestite, gutter cast)	+	+
13. Facies DDV Dolostone with evaporite dissolution vugs Fig. 10E	Dolostone with vugs from the dissolution of evaporites	Dolomicrosparstones	Restricted lagoon Tidal flats Carbonate sabkha	+++	+
10. Facies MC Microbial carbonate Figs. 10F, 14A, B	Gray or white dolomite, frequently with evaporite molds, lamination or stromalolitic domes and variable textures	Dolomicrosparstone. Wackestone to grainstone with intraclasts, peloids and echinoderm	Carbonate sabkha. Tidal flat	+++	++
12. Facies IB Intraformational breccia Fig. 11B	Laminated gray limestone with flat mudstone clasts	Mudstones calcisilstone	Subtidal flat	+	–
11. Facies ML Marl and thin limestone beds with shells Fig. 11C, D	Marl and carbonate alternation, sometimes with mollusk molds or fragments	Mudstone to rudstone with mollusk, echinoderm peloids, foraminifers	Shallow lagoon Pond Tidal flat	+	++
14. Facies OD Ochre dolostone and marl Fig. 11E	Ochre dolomite and marl thin beds with lamination, evaporite molds and carniolar aspect	Mudstone, wackestone to floatstone with mollusks, intraclasts	Evaporitic tidal flat (supratidal)	+	++
15. Facies FL Fine-laminated marly-carbonate Figs. 11F, 14D	Gray carbonate, frequently, with parallel lamination with more or less clay content	Microsparstone Mudstone with peloid intraclast, quartz grain. Silstone	Tidal flat Shallow lagoon Pond	++	++

M1 unit: Lower Muschelkalk; M3 unit: Upper Muschelkalk.
Presence of the facies: −, +, ++, +++, correspond to absent, rare, common, frequent, respectively.

the presence of ghosts of ooids or bioclasts (crinoids) (Fig. 12A, B). Similar facies are common in the Triassic sections of the Betic Cordillera and the Iberian Range, where they are interpreted as calcarenites deposited under high-energy conditions either in shallow waters (shoals) or in tidal channels (Pérez-Valera and Pérez-López, 2008; Escudero-Mozo et al., 2015; Sánchez-Moya et al., 2016). This is also the case in other outcrops of the Iberian Range (Sánchez-Moya et al., 2016), where the presence of a major barrier is not always documented. Oolitic (dolo)wackestone–grainstone with cross-bedding and horizontal laminations, as in the present facies, was described by Adams and Diamond (2019) in the Upper Muschelkalk of Northern Switzerland, interpreted as ooid shoal complexes. These ooid facies are also characteristic of the Upper Muschelkalk of Germany, deposited in shore-parallel belts (Koehrer et al., 2010).

7.4. Bioturbated nodular carbonate (Facies BC)

This facies consists of dark gray muddy nodular dolostone of massive appearance. The original texture of the sediment has been completely destroyed by bioturbation showing a variable nodular texture like a pseudobreccia (bioturbation texture) (Fig. 9E). The observed ichnofossils are small and of low diversity, mostly *Planolites* traces. Also, undulated surfaces and some carbonate beds made up of fine shell-debris occur.

Microfacies. Consisting of dolosparstone, it is probably mudstones in origin (Fig. 12C). The nodular structure related to bioturbation is also visible in thin section.
Interpretation. This facies reflects deposition under low-energy conditions. It is similar to a facies of the Betic Muschelkalk (Pérez-Valera

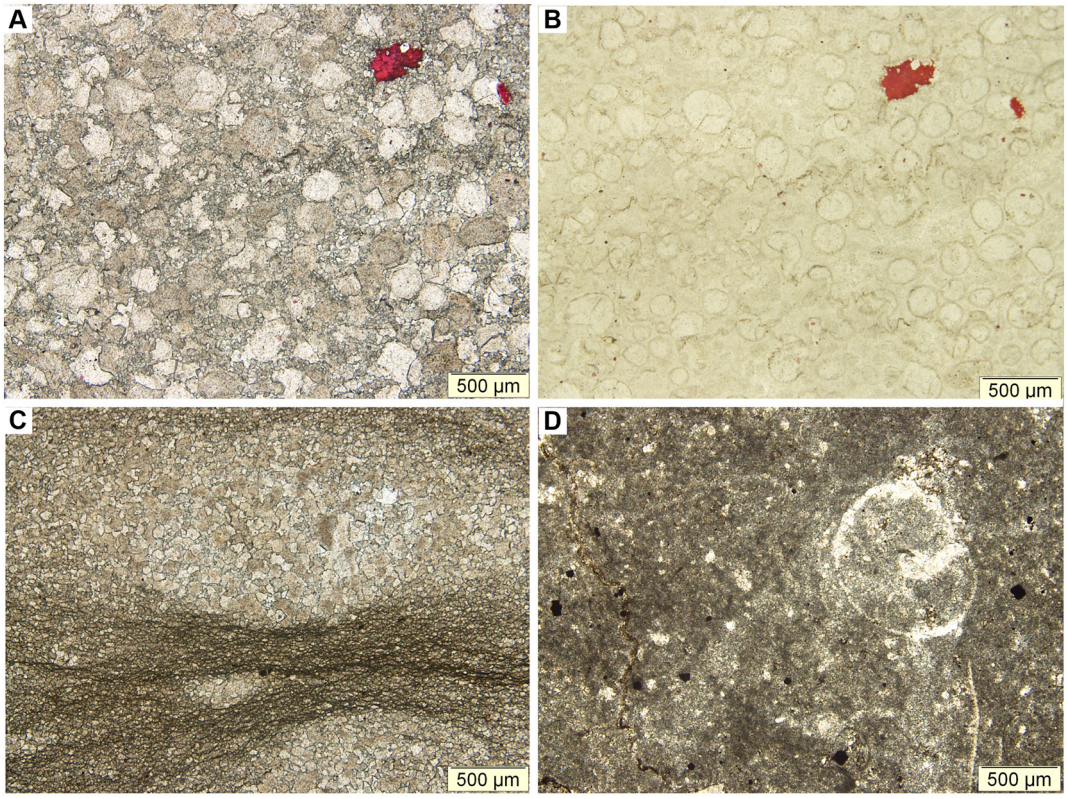

Fig. 12. Photomicrographs of thin-sections. (A) Dolosparite with ooids, visible under cross-polarized light, in the brown dolosparite facies (Facies BD) (red color is calcite) (18–208, Montán A section). (B) The same thin-section with a diffuser (Delgado, 1977) placed under the thin-section for a better view of the ooids. (C) Burrow section of bioturbated carbonate facies in dolomicrosparite (Facies BC) (18–156, Andilla section). (D) Wackestone with bioclasts and small cubic pyrite crystals of paper-thin bedded marly limestone (Facies PT) related to an anoxic environment (15–65, Montán B section). Number of lithologic samples indicated in brackets. (For interpretation of the references to color in this figure legend, the reader is referred to the web version of this article.)

and Pérez-López, 2008), which is interpreted either as offshore deposits, or as lower shoreface sediments affected by storm waves (tempestite bed). Also, this facies can be compared with that described by Knaust (1998) in Germany such as nodular-bedded marlstone of the outer ramp. In NE Netherlands, Pöppelreiter (2002) interpreted bioturbated mudstones to wackestones of nodular texture due to bioturbation as outer ramp deposits.

7.5. Marly limestone with bioturbation (Facies LB)

This facies consists of gray marly limestone beds with bioturbation. The nodular structure is reinforced with increasing bioturbation and clay content (Fig. 9F). Observed ichnofossils are of low to moderate diversity, such as *Planolites* and *Rhizocorallium* ichnogenera (e.g. Knaust, 1998). Locally, bioturbation appears in the upper part of the beds, and wave ripples appear at the bed tops.

Microfacies. This consists mainly of mudstone, although wackestone with mollusk fragments (bivalves, gastropods) and some echinoderm debris occur.
Interpretation. The facies can be interpreted as moderately bioturbated, subtidal deposits of tidal flats (Shinn, 1983). These deposits correspond to very shallow sediments that were probably deposited just below the fair-weather wave base. They may also reflect depositional conditions (softgrounds) in varied settings such as quiescent bays or lagoons (Gingras et al., 2009). In this facies, it is possible to define shallowing upward sequences. Similar facies with none to moderate bioturbation have been described by Adams and Diamond (2019) and interpreted as low-energy subtidal lagoon deposits in the Upper Muschelkalk of Northern Switzerland. The influence of waves or storms in these sediments varies from one area to another and produces wave-generated bed forms and, locally, tempestite beds. The facies can be correlated with some lithofacies of the 'fucoides' bioturbation member (Vilella Baixa unit) of the lower Muschelkalk in the Triassic Catalan Basin, which were interpreted as shallow-subtidal deposits (Ramón and Calvet, 1987; Calvet et al., 1990).

7.6. Paper-thin bedded marly limestone (Facies PT)

This facies occurs mainly in the upper Muschelkalk unit. It consists of argillaceous dark gray marly limestone with characteristic paper-thin bedding (Fig. 10A) forming bed packages 0.5 to 5 m thick. Texture is very monotonous without any type of bioturbation and, only locally, some isolated bivalves (*Modiolus*) appear. Evaporitic marly dolostone and fine-laminated dolostone (facies OD) overlie the facies in some sections. In others, however, the overlying beds are bioclastic limestones.

Microfacies. It is mudstone with some gastropods and/or silt grains of quartz. Pyrite crystals appear in some thin section (Fig. 12D).
Interpretation. The very fine-grained homogenous texture of this facies is interpreted as very low-energy deposits. The dark gray color and lack of bioturbation may suggest suboxic conditions. A similar facies has been described in the Cretaceous, as a Modiolus biofacies, in which this species appears alone in the muddy, low-energy, oxygen-poor bottom (Lazo, 2007). In the Betic Cordillera, this facies is characteristic of areas closer to the continent, as it is not present in the paleogeographic units farther away from the basin edge (Pérez-

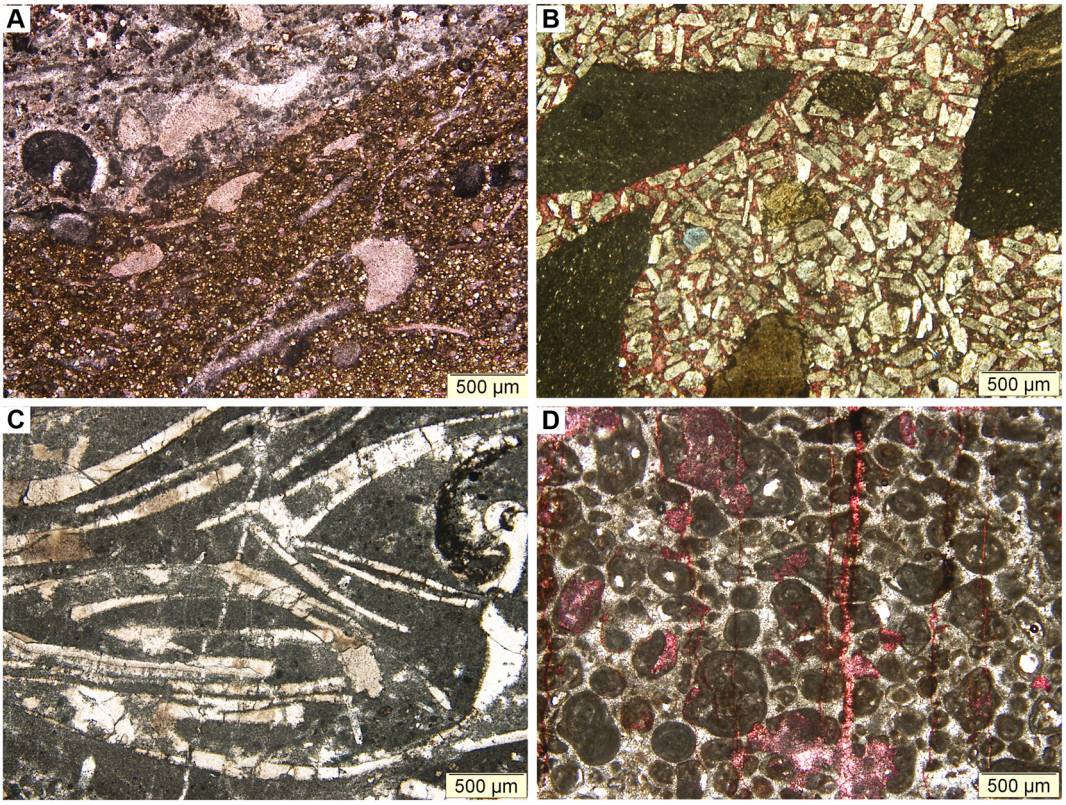

Fig. 13. Photomicrographs of thin-sections. (A) Wackestone featuring *Balanoglossites* (Facies BL) with a reworked packstone interval (upper left) and small ochre ferroan dolomite crystals (16–117, Paraíso section). (B) Crinoid grainstone with lutite clasts of the polymictic breccia (Facies PB), which corresponds to a transgressive lag deposit. Calcite cement appears red (18–113, Fuente La Reina section). (C) Tempestite mollusk rudstone of the lower carbonate-marl alternation (18–143, Andilla section). (D) Tempestite grainstone with intraclasts, ooids and grapestones deposited in the lower shoreface zone indicating the presence of ooids in the Anisian shallower platform (Facies SD) (15–83, Arteas section). Number of lithologic samples indicated in brackets. (For interpretation of the references to color in this figure legend, the reader is referred to the web version of this article.)

Valera and Pérez-López, 2008). Accordingly, it is interpreted as shallow, restricted lagoon deposits, with some siliciclastic input. In the present study, the gradual transition into carniolar carbonates or shallower intertidal deposits (facies OD, DDV or MC) observed in some sections enables us to interpret these sediments as deposited in a very shallow, restricted water mass (anoxic conditions) near the coastal flat.

7.7. Bioclastic limestone with Balanoglossites (Facies BL)

In some sections, gray bioclastic limestone beds occur, 20 to 50 cm thick, containing ochre ferroan dolomite within burrows (Fig. 10B). Generally, they are uncommon in the successions and can be used as discrete marker beds. The ochre dolomite corresponds to fillings of *Balanoglossites* burrows (Knaust, 2007). This facies often displays coarsening-upwards, graded bedding with bioclastic rudstones at the top. Commonly, the bed top is an erosive, irregular-to-undulated surface that cross-cuts the burrows. These top surfaces display iron mineralizations and *Trypanites* burrows locally.

Microfacies. The bioclastic deposits of this facies are formed by wackestone to packstone/rudstone with bivalves, gastropods, echinoderms and peloids (Fig. 13A). The bioclasts can be very fragmented and some gastropods may be filled with a micritic sediment different from that of the matrix, indicating the grain transport.
Interpretation. This facies is interpreted as shallow water deposits in subtidal zones or very shallow lagoons with upward-increasing energy, which usually form shallowing-upward sequences, locally, with an erosional surface at top. These surfaces, with iron mineralizations and *Trypanites* burrows, are interpreted as a (hard-) firm ground (Knaust, 2007). These hard surfaces, with *Balanoglossites* burrows, are common in the European Muschelkalk facies (Knaust and Costamagna, 2012) in relatively proximal settings. In the present study, some beds of this facies contain reworked fossils and might be the result of storm reworking (Costamagna and Barca, 2002; Pérez-Valera and Pérez-López, 2008). Burrows are often filled with coarse-grained sediment, which could be associated with storms or downward shifts of the sea level (Handford and Loucks, 1993).

7.8. Polymictic breccia (Facies PB)

This facies consists of polymictic breccia with sediment fragments of different lithologic nature, mainly angular carbonate fragments and clay rip-up clasts. The fragments or clasts vary in size from a few millimeters to about 10 cm. The facies has a bioclastic grainstone matrix of crinoid ossicles. This breccia appears in the lower part of few sections of the lower Muschelkalk unit, forming thin beds (15–30 cm thick) with erosive bases (Figs. 10C, 13B). The thin beds overlay stromatolite beds (facies MC) via a sharp erosive contact. Generally, wave surfaces are present at the top of these breccias.

Microfacies. It consists of grainstone/rudstone with crinoids. Lutite and carbonate clasts can be observed in thin section.
Interpretation. This type of breccia is very peculiar because of its features and because it only appears at the base of some sections of the lower Muschelkalk (Fuente la Reina and Torralba del Pinar sections). It is interpreted as transgressive lag deposits in tidal flats based on its position in the successions and on the presence of clay angular clasts (Van Wagoner et al., 1990; Cattaneo and Steel, 2003). The crinoid fragments come from a high energy littoral zone of a ramp in the

initial stages of flooding (Zamora et al., 2018), indicating a transgressive trend. These breccias deposited during the first ingressions were probably produced or favored by storms. Kolar-Jurkovsek et al. (2021) describe, in the Lower Triassic deposits, bioclastic lags related to sediments on a shallow epicontinental ramp with pronounced long-term transgression for the Lower Triassic deposits, with storm events.

7.9. Shell-debris limestone (Facies SD)

This facies appears as an intercalation between several of the facies described in this study. It consists of bioclastic thin beds (2 to about 15 cm thick) with current sedimentary structures. Some of these beds show graded and/or parallel lamination and erosive bases. Locally, they show hummocky cross-stratification (Arteas section) and appear mainly as intercalations within fine-grained mud sediments (Fig. 10D).

Microfacies. The textures vary from packstone and floatstone to grainstone and rudstone with fragments of bivalves, gastropods and echinoderms, and also locally with peloids, intraclasts, ooids and quartz grains (Fig. 13C, D).

Interpretation. This facies shows characteristic features of tempestites (e.g., Kreisa, 1981; Aigner, 1985; Pérez-López and Pérez-Valera, 2012), mainly of high energy texture, current structures and in beds with erosive bases which occur between muddy deposits. It is interpreted as storm beds formed in the lower shoreface ("offshore transition zone"). It also is interpreted as formed in restricted lagoons where reworking during storm events, formation of bioclastic beds, and winnowed storm deposits occurred (Pérez-López and Pérez-Valera, 2012). Tempestite beds deposited in lower shorefaces (mid ramp) are frequent in the upper Muschelkalk of the Germanic Basin (e.g., Aigner, 1985; Adams and Diamond, 2019), as well as in the Anisian ramp of the Western Balkanides (Chatalov, 2013) or Middle Triassic of the Polish Tatra Mountains (Jaglarz and Szulc, 2003).

7.10. Dolostone with evaporite dissolution vugs (DDV)

In several sections, dolostone with vugs caused by the dissolution of evaporite (anhydrite) occur. The facies consists of thin cream-white beds (5 to 15 cm thick) with calcite-filled vugs (Fig. 10E). Locally, it displays horizontal lamination. In some sections this facies presents wave bedding of diagenetic origin, as undulating bedded carbonate (Facies UBC).

Microfacies. It is dolomicrosparstone. No grain type is observed in thin section, only some small pores filled with calcite crystals.

Interpretation. This facies is interpreted as tidal or intertidal pond deposits in arid conditions, related to carbonate sabkha, mainly, in the case of the lower Muschelkalk. A similar facies related to sabkha environments has been described in some Keuper deposits (Ortí et al., 2018). The thin lamination of this facies is interpreted as tidal deposits and microbial mats. In the upper part of the Muschelkalk successions of northern Switzerland, Adams and Diamond (2019) described laminated dolomudstone with wave-ripples, sulfate nodules and flat-pebble conglomerates as intertidal microbial laminites in the progradation of the shore deposits.

7.11. Microbial carbonate (Facies MC)

This facies is characteristic of the top of the lower Muschelkalk unit, although it is also present in the upper Muschelkalk unit (Manzanera section). It consists of gray, cream-white dolostones or marly-dolostones bearing microbial lamination. Several types of microbial carbonates such as microbial mats, stromatolites, and wide domes can be distinguished (Figs. 10F, 11A). Locally, these laminated or domal dolostones bear breccia intercalations and beds with evaporite molds (facies DDV).

Microfacies. This microfacies often consists of dolomicrosparstone. It may also contain mudstones, thin laminated wackestones or pelletal grainstones with intraclasts (Fig. 14A). Also, ooids, echinoderm fragments, and intraclasts are identified in thin-section (Fig. 14B).

Interpretation. Lamination and irregular undulated morphology are typical of films and layers of cyanobacteria and fungi growing on the sediment surface as microbiolaminites and stromatolites (Walter, 1976). This type of facies is interpreted as shallow, low-energy, inter-to-uppermost subtidal stromatolites (Jahnert and Collins, 2012) and even as supratidal stromatolites (Zhang et al., 2019). In the samples examined, the presence of echinoderms supports this subtidal interpretation, while the presence of breccias suggests carbonate supratidal flats and the dolostones with evaporite molds indicate arid conditions. Accordingly, this facies is interpreted as deposits of a peritidal zone under the influence of storms, sometimes associated with carbonate sabkha environments. Stromatolites are well developed in the Germanic Basin and occur in other Triassic units as the Röt and the Middle Muschelkalk (Szulc, 1997) in highstress environments. In the Buntsanstein of the Harz Mountains (Germany), stromatolites are associated with storm ooid deposits in playa-lake environments (Paul and Peryt, 2000).

7.12. Intraformational breccias (Facies IB)

This facies consist of gray limestone with lamination and abundant levels of intraclasts (Fig. 11B). The levels are breccias formed mostly by cm-sized flat-pebbles of micrite. Commonly the boundaries of the flat-pebbles are not sharp and have a shape that can be mistaken for bioturbation (pseudobreccia). The smooth boundaries of these intraclasts indicate they were semiconsolidated (soft) during deposition. This facies appears in the lower Muschelkalk units (Fuente la Reina and Torralba sections).

Microfacies. The microfacies texture of pebbles consists of mudstone and laminated calcisiltstone. No grain type is observed.

Interpretation. This muddy facies displaying thin lamination is interpreted as subtidal deposits with intraclasts due to reworking of muddy sediment during storms. In general, the carbonate conglomerates with intraclasts are interpreted as supratidal, intertidal and subtidal deposits although they are more common in the intertidal zone (e.g., Flügel, 2004: Shinn, 1983; Matysik, 2019). However, this facies has peculiar features which are characteristic of anachronistic carbonate facies documented in the Lower Triassic, greatly resembling Precambrian and Lower Paleozoic analogs (Wignall and Twitchett, 1999; Chatalov, 2017). This facies is very similar to those described by Chatalov (2017) in the Lower Triassic rocks of western Balkanides, interpreted as subtidal sediments. The breccia is the result of erosion and reworking by storm-induced currents or by seismic shock (Chatalov, 2017). Similar facies were described also within the laminated limestone of the upper Muschelkalk of the Betic Cordillera by Pérez-Valera and Pérez-López (2008). The latter authors interpreted this facies as shallow nearshore deposits, from a subtidal to intertidal zone due to the presence of small channels. In conclusion, this facies of Eastern Iberia, in which laminated micrites alternate with breccia levels of flat and semi-consolidated clasts in total absence of emersion features, desiccation cracks or fenestral structures, can be considered as low-energy subtidal deposits, sometimes affected by storms or seismic shock, during the Anisian age.

7.13. Marl and thin limestone beds with shells (Facies ML)

This facies is one of the most common in the Muschelkalk units examined. It consists of thin muddy bioclastic limestone beds

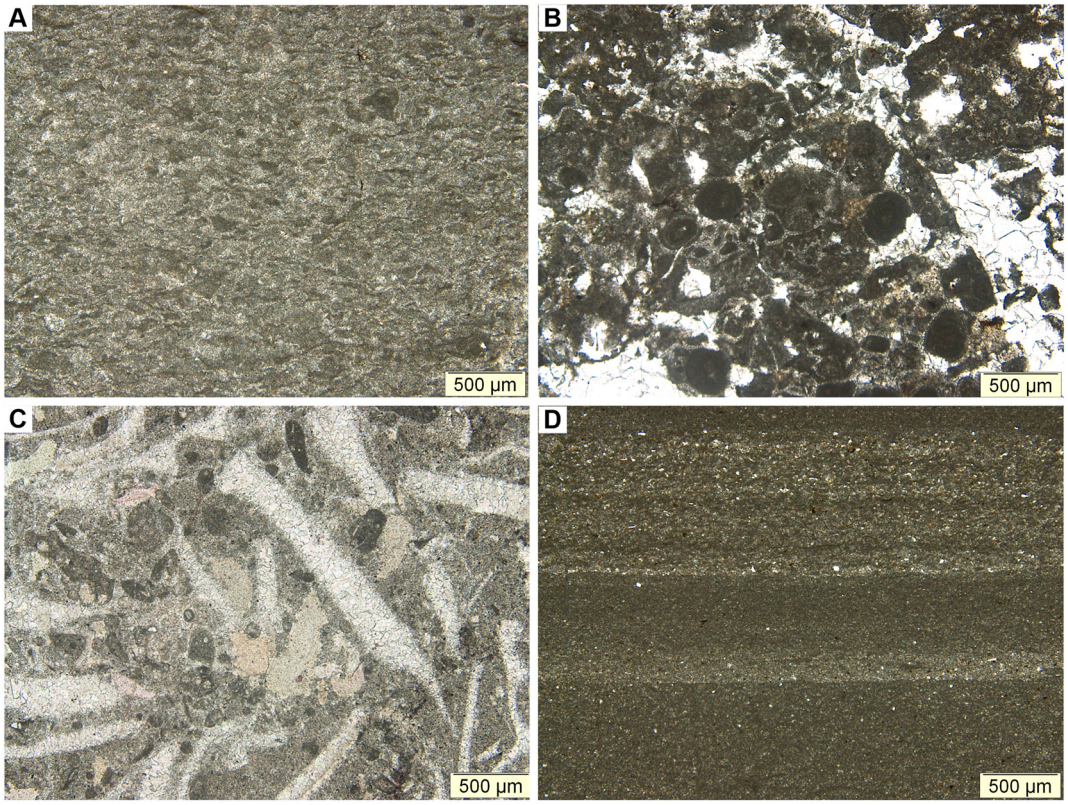

Fig. 14. Photomicrographs of thin-sections. (A and B) Microfacies of the 'terminal carbonate complex' which locally consist of (A) mudstone or wackestone-packstone with abundant peloids and intraclasts (15–99, Arteas section) or (B) brecciated packstone with intraclasts, ooids and peloids (17–88, Arteas section). (C) Packstone with mollusks, crinoids, intraclasts and peloids which corresponds to shell-debris limestone (Facies SD) (18–141, Paraíso section). Note the broken mollusks shells that could indicate several storm episodes. (D) Laminated calcisiltite with quartz fine grains of small lagoon or pond deposits. This microfacies appears in fine laminate carbonate between marl (Facies FL) (17–43, Arteas section). Number of lithologic samples indicated in brackets.

(2 to 15 cm thick) in alternation with gray or creamy marls (Fig. 11C). The limestone beds contain bioclasts, mainly of bivalves and gastropods. Bivalve molds filled with micrite or sparite cement are also observed in some beds (Fig. 11D) and some mollusk bioclasts also occur in the marls. Bioclast or shell contents are quite variable from one bed to another or from one section to another, and are locally absent. The most characteristic bivalve shells correspond to *Pseudocorbula gregaria* (Münsteri) and also to *Bakevellia costata* (Schlotheim). Locally, this facies has shell-debris limestone (Facies SD) and/or bioclastic limestone containing *Balanoglossites* (Facies BL).

Microfacies. Microtexture is very variable spanning from mudstone to rudstone with mollusk and echinoderm fragments, and peloids (Fig. 14C). In some sections of the upper Muschelkalk unit, the microfacies of the bioclastic beds shows the foraminifer *Nodosaria ordinata* (Trifonova) associated with mollusk fragments, intraclasts and peloids (wackestone/floatstone).
Interpretation. This alternation of marl and limestone beds, locally bearing shells or bioclasts, is interpreted as very shallow-marine sediments deposited under lagoon conditions or in pond environment. In general, the facies suggests a low-energy setting related to the nearshore and to high-energy storm deposits, frequently winnowed tempestites in which shell fragments form graded beds or erosive bases (Pérez-López and Pérez-Valera, 2012). Similar lithologies and fossil contents have been observed at the top of the upper Muschelkalk unit in different sections of the Iberian Peninsula (Pérez-Arlucea, 1991; Pérez-López et al., 1991; Márquez-Aliaga and Ros, 2003; Escudero-Mozo et al., 2016). Siliciclastic sediment input results in marly beds intercalated between bioclastic limestones.

7.14. Ochre dolostone and marl (Facies OD)

This facies consists of ochre dolostone beds alternating with marls (Fig. 11E). Locally, the beds are laminated and display molds of gypsum crystals, tepee structures or desiccation cracks. Locally, the bioclastic carbonates display some current structures (graded bedding or lamination) which can be associated with the facies SD (shell-debris limestone). Porosity in these carbonates can be abundant giving way to a carniolar appearance.

Microfacies. It is mainly dolomicrosparstone (mudstone), although wackestone/floatstone with mollusk fragments and intraclasts can be also observed.
Interpretation. Facies exhibiting these sedimentary structures are typical of intertidal–supratidal deposits, although the bioclastic bed intercalations are related to lagoon or pond deposits. Some of these beds are interpreted as storm deposits when current structures are present. The irregular lamination can be associated with algal mats, and the gypsum molds indicate arid conditions in a tidal flat setting (Pratt and James, 1986; Pérez-Valera and Pérez-López, 2008). This facies is frequent in the upper part of the successions, where it passes to the coastal mud deposits of the Keuper facies or of the middle Muschelkalk. In the Middle Triassic of Netherlands, Germany or Sardinia, similar or correlated facies have been described in the upper parts of the successions (e.g., Rameil et al., 2000; Pöppelreiter, 2002; Knaust and Costamagna, 2012).

7.15. Fine-laminated carbonate (Facies FL)

Marly limestone or dolostone with fine lamination occurs in some centimeter- to decimeter-thick beds containing variable amounts of

clay (Fig. 11F). This facies mainly occurs in the lower part of the studied sections, although it can occur also in any part of the succession. This facies is similar to the microbial carbonate facies (CC), although here, fine clastic components are more abundant.

Microfacies. The microfacies is microsparstone, but also mudstone with some intraclasts, peloids, and small quartz grains is observed. In addition, some thin beds of laminated calcisiltstone bearing quartz grains alternate with the mudstones (Fig. 14D). Fenestral porosity and small evaporite molds are observed locally.
Interpretation. These deposits exhibiting fine lamination are interpreted as sediments of mixed tidal flats. Lamination could point to microbial mats such as those found today on the Persian Gulf coast (Kendall and Skipwith, 1968). Similar planar-laminated stromatolites present at the base of the upper Muschelkalk unit in the Triassic Catalan Basin (Rojals unit, NE Spain), were interpreted as intertidal deposits by Calvet et al. (1990). The alternation of calcisiltstone and micritic mudstone in this facies indicates fluctuating hydrodynamic conditions related to a tidal flat setting, or also to fine sediments deposited in small, shallow lagoon or pond environments. The sporadic presence of fenestral pores is also related to tidal flat deposits (Flügel, 2004). Based on the thinness of these beds, the tidal flats were much less developed than those in the upper part of the studied sections (MC facies).

8. Facies associations and sedimentary environments

The previously described facies of the Iberian Muschelkalk units are grouped into seven genetically linked lithofacies associations (FA). The results of the present study do not lead to the interpretation of a standard platform model. It is necessary to make the interpretation under different aspects according to the precision that can be achieved from the sedimentary environment interpretation. These facies associations can be arranged according to the following considerations:

- Sedimentary environments with specific depositional conditions (e.g., Reading, 1996): coastal plain, sabkha, pond, tidal flat (supratidal, intertidal or subtidal), shoal, lagoon.
- Sedimentary zones contextualized in the marine domains in relation to the fair weather wave base and storm wave base (Mac-Lane, 1995; Nichols, 2009): Upper shoreface, lower shoreface (or offshore-transition) and offshore, where the lower shoreface or offshore-transition zone is the shelf area between the fair weather and storm wave bases.
- Sedimentary environments with a wide range according to the type of carbonate platform (Read, 1985; Nichols, 2009): ramp and rimmed shelf

8.1. FA1 - carbonate sabkha

The thick packages of light-colored (creamy white) carbonates with evaporite molds, dissolution vugs (Facies DDV) of anhydrite nodules, stromatolites, domes and breccias (Facies MC)are interpreted as carbonate sabkha deposits (Ortí et al., 2017). These facies suggest arid conditions of deposition where breccias or stromatolites can develop in different ways. In some sections, this lithofacies association bears polymictic breccia (facies PB). There is little or no supply of siliciclastic materials in these environments. In many cases, this facies association will significantly mark the end of the lower Muschelkalk deposits.

A similar facies association can be observed, for example, in the upper Muschelkalk of Germany (e.g., Szulc, 1999). However, it usually has a more detrital or siliciclastic character than in the present study. In an interesting study of the Middle Triassic, Diedrich (2009) related the different facies of tidal flat and sabkha deposits, some similar to those occurring in Eastern Iberia.

8.2. FA2 – tidal flat

This lithofacies association consists of the thin laminated carbonates of facies FL, occasionally, with some thin beds of brown dolosparite facies (BD)interpreted as tidal channels. This facies may have some input of siliciclastic material with the development of more marly deposits in small lagoons or ponds associated with tidal flats. The facies association was observed to vary between the different sections. Marl beds or microbial carbonate facies (MC) were more or less developed. Laminated carbonate with vugs from evaporites can be present (DDV) indicating arid conditions . Also, ochre dolomite and marl (OD) can be present. All these are deposits of intertidal–supratidal environment similar to the "cavernous limestones" (Szulc, 2000) of the upper part of the Germanic lower Muschelkalk, interpreted as restricted inner ramp (lagoon) deposits characterized by frequent emersion events (Bodzioch and Kwiatkowski, 1992).

8.3. FA3 – lagoon

The lithofacies association that characterizes lagoons is mainly mudstones and wackestones with scarce or moderate bioturbation (Facies LB), although other facies can be present depending on the variable lagoon conditions. The lagoons could have been restricted and more or less deep. Also, they could have been partially connected to the open sea. This means the lagoons could be affected by storms or have a higher oxygen content in their waters and consequently more organisms could live there.

It was observed that the sediments deposited between tidal flat environments and high energy shoals (facies BD) correspond to different sediment types depending on the section or outcrop studied. For example, the bioclastic beds containing *Balanoglossites* (BL) are lagoon deposits or also marl and thin limestone beds with shells (ML). In these cases, shell-debris limestones (SD) can occur, which are interpreted as storm deposits. In more restricted conditions, paper-thin bedded marly limestone (PT) occurs, or intraformational breccias (IB) in shallower water. The variety of facies is explained by changing depositional conditions in the lagoon both in space and time. In the Triassic literature it is possible to find several types of facies association assigned to lagoon environments (e.g., Adams and Diamond, 2019; Pöppelreiter, 2002).

8.4. FA4 – shoal complex

This facies association consists mainly of brown dolostone (BD) with different crystal sizes in which ooids or crinoids were identified in the microfacies formed by larger dolomite crystals. The presence of intertidal facies with evaporite molds should be noted also (MC facies). This association shows massive beds from 8 to 30 m thick, with current sedimentary structures and/or evaporite molds. The dolosparite thickest beds have erosive bases and the thinnest beds show horizontal or small ripple lamination. These deposits are interpreted as a shoal complex of varying development, being thicker in the upper Muschelkalk. The associated fine-grained, laminated deposits, and the evaporite molds indicate significant changes in energy conditions, probably due to the formation of tidal flats, locally with ponds, related to a shoaling process or bar emersion that was able to protect some zones of the platform. These features suggest the sedimentary environment was very shallow and remained exposed for long periods of time. This facies association is more frequent in the Triassic basins of central Europe. Depending on the situation, barrier deposits can show different extents or thickness (e.g., Vecsei and Duringer, 2003).

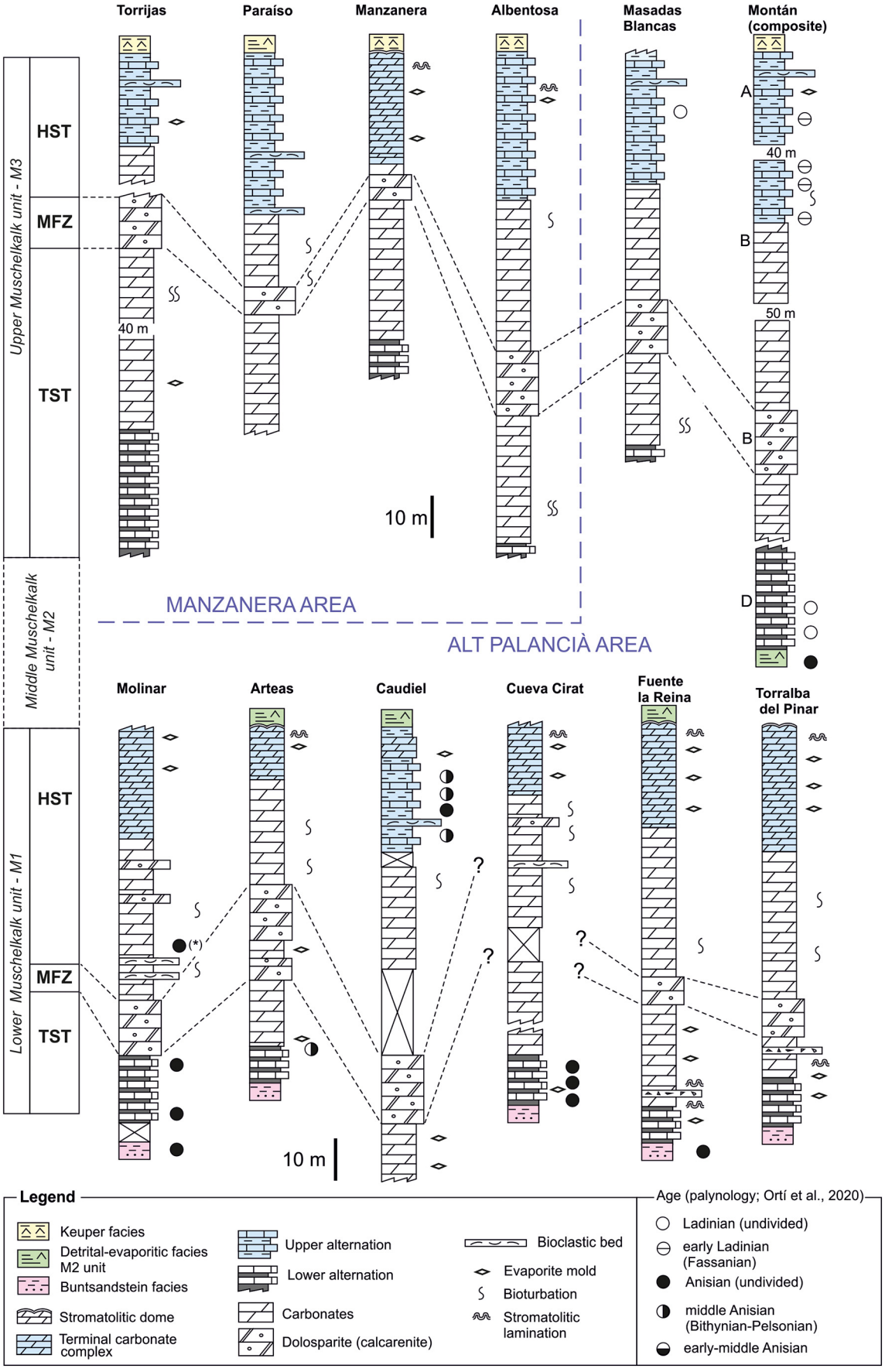
Torrijas
Paraíso
Manzanera
Albentosa
Masadas Blancas
Montán (composite)
Upper Muschelkalk unit - M3
HST
MFZ
TST
40 m
10 m
A
B
50 m
B
D
MANZANERA AREA
ALT PALANCIÀ AREA
Middle Muschelkalk unit - M2
Lower Muschelkalk unit - M1
Molinar
Arteas
Caudiel
Cueva Cirat
Fuente la Reina
Torralba del Pinar
HST
MFZ
TST
(*)
?
?
?
10 m
Legend
Keuper facies
Detrital-evaporitic facies M2 unit
Buntsandstein facies
Stromatolitic dome
Terminal carbonate complex
Upper alternation
Lower alternation
Carbonates
Dolosparite (calcarenite)
Bioclastic bed
Evaporite mold
Bioturbation
Stromatolitic lamination
Age (palynology; Ortí et al., 2020)
Ladinian (undivided)
early Ladinian (Fassanian)
Anisian (undivided)
middle Anisian (Bithynian-Pelsonian)
early-middle Anisian

8.5. FA5 – upper shoreface zone

The facies taking up part of the upper shoreface zone is basically thin-bedded carbonate (TB) with gutter casts, some cross-stratification and erosive channels. These sediments were deposited in a muddy ramp which was more influenced by tides than waves, and behaved as a bypass zone in deposition during storms, forming gutter casts (Myrow, 1991; Pérez-López, 2001; Pérez-López and Pérez-Valera, 2012). Duringer and Vecsei (1998) described similar facies as subtidal deposits of very shallow water in the Upper Muschelkalk of the W Germanic Basin. In some zones of this ramp, the mud sediment consisted of silt-sized grains as suggested by Vecsei and Duringer (1998).

8.6. FA6 – lower shoreface zone

This facies association characterizes the main deep deposits which are formed by undulating bedded carbonate (UBC). Locally, also bioturbated carbonate (BC) with a nodular structure and storm deposits occur (facies SD), although they are not abundant or common.

8.7. FA7 – offshore zone

This facies association can be reduced to the presence of nodular bioturbated facies (facies BC). It forms a massive homogeneous package of either a breccia-like appearance (pseudobreccia) or comprises nodules bounded by pressure-dissolution surfaces. Relatively deeper deposits, which are not affected by storm surges, can be considered. It should be highlighted that this facies only appears in some of the upper Muschelkalk sections. As indicated above, similar facies of the Central Europe Triassic have been interpreted as offshore deposits (e.g. Knaust, 1998; Pöppelreiter, 2002).

9. Facies and sea-level changes

The vertical arrangement of the facies associations in the studied sections (Figs. 4 to 8) allows for the identification of a distinct transgressive–regressive sequence in the two Muschelkalk units (Figs. 15, 16, 17). Moreover, two transgressive and two regressive phases can be differentiated in each of the trangressive–regressive sequences.

9.1. First transgressive phase

This phase corresponds to the lower carbonate-marl alternation in the two Muschelkalk units. In each section, the facies association is different, although the tidal flat facies (FA2) predominates. It is characterized mainly, but not exclusively, by the diagnostic FL facies at the base. In some sections (Arteas, Molinar), however, the facies association FA3 (lagoons, ponds) appears in this phase. Deepening-upward cycles at the meter-scale are distinguished in this lower alternation (A cycle, Figs. 16, 17), and are made up of marly intervals below and by fine-laminated marly-carbonate beds (FL facies) above, the latter facies locally showing undulated laminations. In this case, the marls are interpreted as shallower deposits because they are equivalent to the coastal deposits of Röt facies or of the middle Muschelkalk lutites which outcrop at the base of the lower and upper Muschelkalk, respectively. Therefore, the FL facies are the first carbonate beds that appear at the base of the Muschelkalk successions, mainly in the upper Muschelkalk unit.

In the lower Muschelkalk unit, facies association FA1 of sabkha setting is also present. Stromatolitic dolostones (MC facies) are common and, occasionally, polymictic breccias (PB facies) also appear. These breccias of lag deposits (Fig. 10C) occur in the Fuente la Reina section (Alt Palància area) and Torralba section (Espadà Ridge) defining the deepening-upward B cycle (Fig. 16). This cycle begins with marls of the Röt facies overlain by the first tidal carbonates. On top of these carbonates, the facies of breccia lag can appear (facies PB). In these two sections, the lower carbonate-marl alternation (up to 11–13 cycles) of the transgressive phase is followed by the deposition of mudstones of the tidal flat (FA2) setting.

The lower carbonate-marl alternation corresponds to a mixed tidal flat of low energy conditions in a ramp context for the two Muschelkalk units. This alternation is overlain by subtidal deposits characterized by variable facies (FA3 and FA3) and deeper sediments of the lower shoreface (AF6) including tempestites (Arteas section, Fig. 5), and, locally, offshore facies (AF7). In the sediments of the upper shoreface (FA5) intraformational truncation surfaces, slumps and gutter casts occur (Fig. 17A) mainly in the Torrijas section (Fig. 8), indicating a gentle ramp slope (Read, 1985; Knaust, 2000; Pérez-López and Pérez-Valera, 2012).

9.2. Second transgressive phase

Variable facies occur during the second transgressive phase, the most significant being brown dolosparite (BD facies), which corresponds to the most energetic deposits (mainly calcarenites) of the transgressive sequence. These coarser sediments indicate some connection of the ramp with the open sea resulting in a change of the energy regime (Figs. 16B, 17B). However, these sediments were not coeval in all the sections examined and were formed in different settings, in a foreshore and/or shoreface zone. In fact, some of them grade laterally (FA4) into bioturbated sediments of nearby lagoons (BC facies), and others into laminated and fine sediments (FL facies) of tidal flats (C cycles; Fig. 16B). Moreover, the brown dolosparites bear laminated limestone in some sections indicating restricted tidal flats and lagoons due to shoaling processes. These settings were slightly more restricted in the lower Muschelkalk than upper Muschelkalk unit. Overlying the calcarenites (BD facies), the bioturbated carbonates (BC facies), which also indicate shallow-marine environment deposits of low energy, are predominant in the lower Muschelkalk unit, while the thin-bedded carbonate and marls (TB facies) are most frequent in the upper Muschelkalk unit (C′ cycles; Fig. 17B). Therefore, it can be assumed that the platform morphology became a rimmed shelf during the second transgressive phase in the lower Muschelkalk unit, while it remained as a ramp with shoals in the upper Muschelkalk unit.

The maximum flooding zone (mfz) is recognized by the change from long-term transgression to long-term regression within the different lithostratigraphic units. The presence of shallowing upward cycles overlying the calcarenites (BD facies) and associated marly deposits of the first regressive phase suggests that these calcarenite facies represent this zone. It should be noted that this is a relatively low-energy muddy ramp, and there are no high-energy deposits close to the shore in the first stages. The only sandy carbonate deposits are those corresponding to the brown dolostone (BD) facies. Therefore, it is interpreted that these are the sediments that represent those of the maximum transgression, when the sea level could have overflowed the possible barriers (islands) that stopped the higher energy of the fair weather waves.

Fig. 15. Correlation of sections representative of the lower and upper Muschelkalk units. The lower carbonate-marl alternation and the assemblage of the upper carbonate-marl alternation and the 'terminal carbonate complex' are highlighted. TST: trangressive system tract; MFZ: maximum flooding zone; HST: highstand system tract. In the Alt Palància area, the age of the sub-units is based on the palynological data provided in Ortí et al. (2020). In the Molinar section (*), the Anisian age is also based on the presence of the crinoid *Holocrinus dubius* (Goldfuss) (see Table 1).

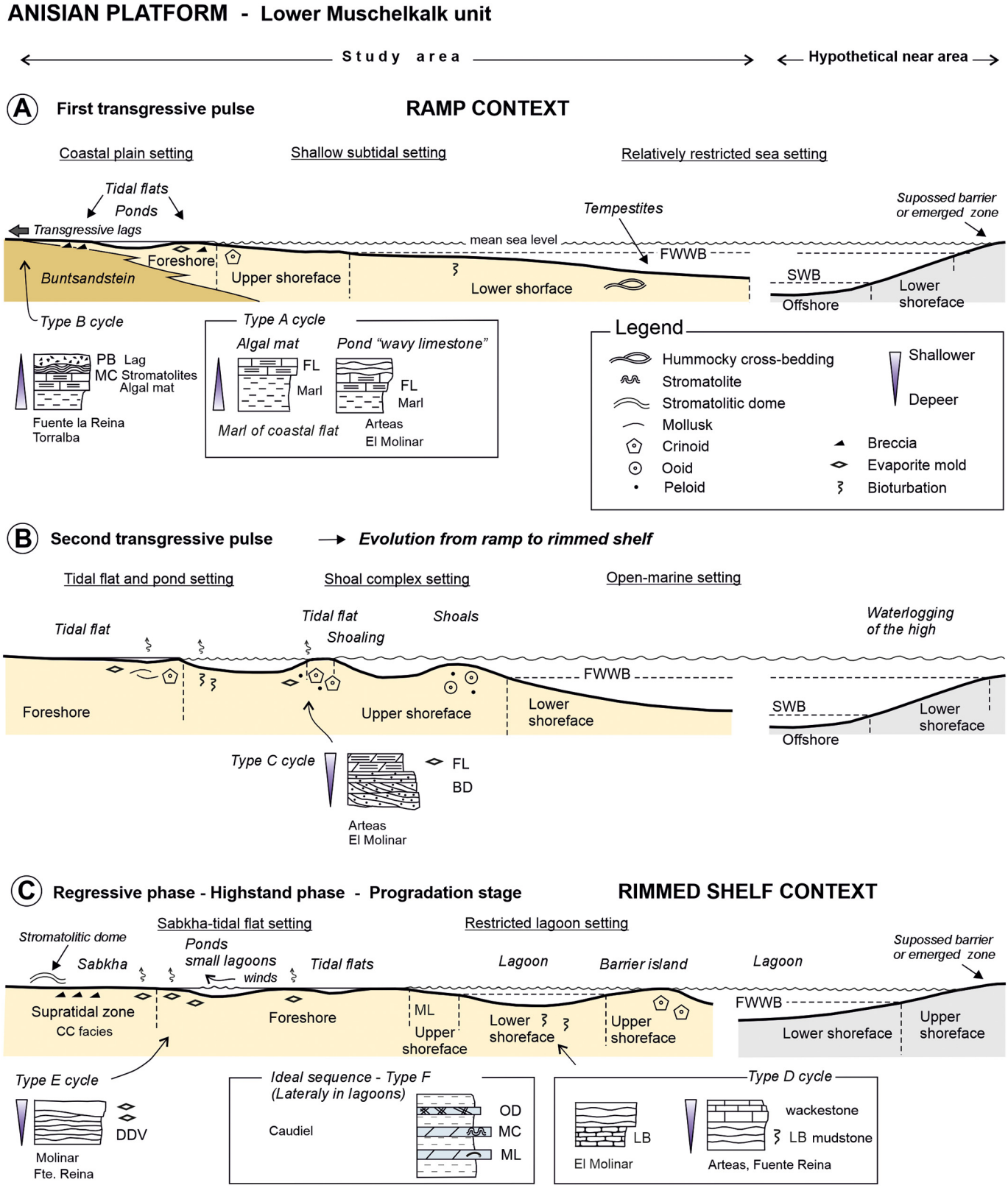

Fig. 16. Environments and platform model for the lower Muschelkalk unit (Anisian). (A) First transgressive pulse in a ramp context. (B) Second transgressive pulse during the development of calcarenite shoals locally containing tidal flats. (C) Regressive phase when carbonate sabkhas became established in very restricted environments ('terminal carbonate complex').

9.3. Initial regressive phase (early highstand)

The initial regressive phase in the two Muschelkalk units coincides with the highstand stage in which sedimentary deposits prograde towards the sea (e.g. Bertram, 2012). In the study areas, this phase is not documented by a distinct interval in the lower Muschelkalk unit, while it is clearly marked by a stromatolite bed (MC facies) in the upper Muschelkalk unit. The most significant facies association of this

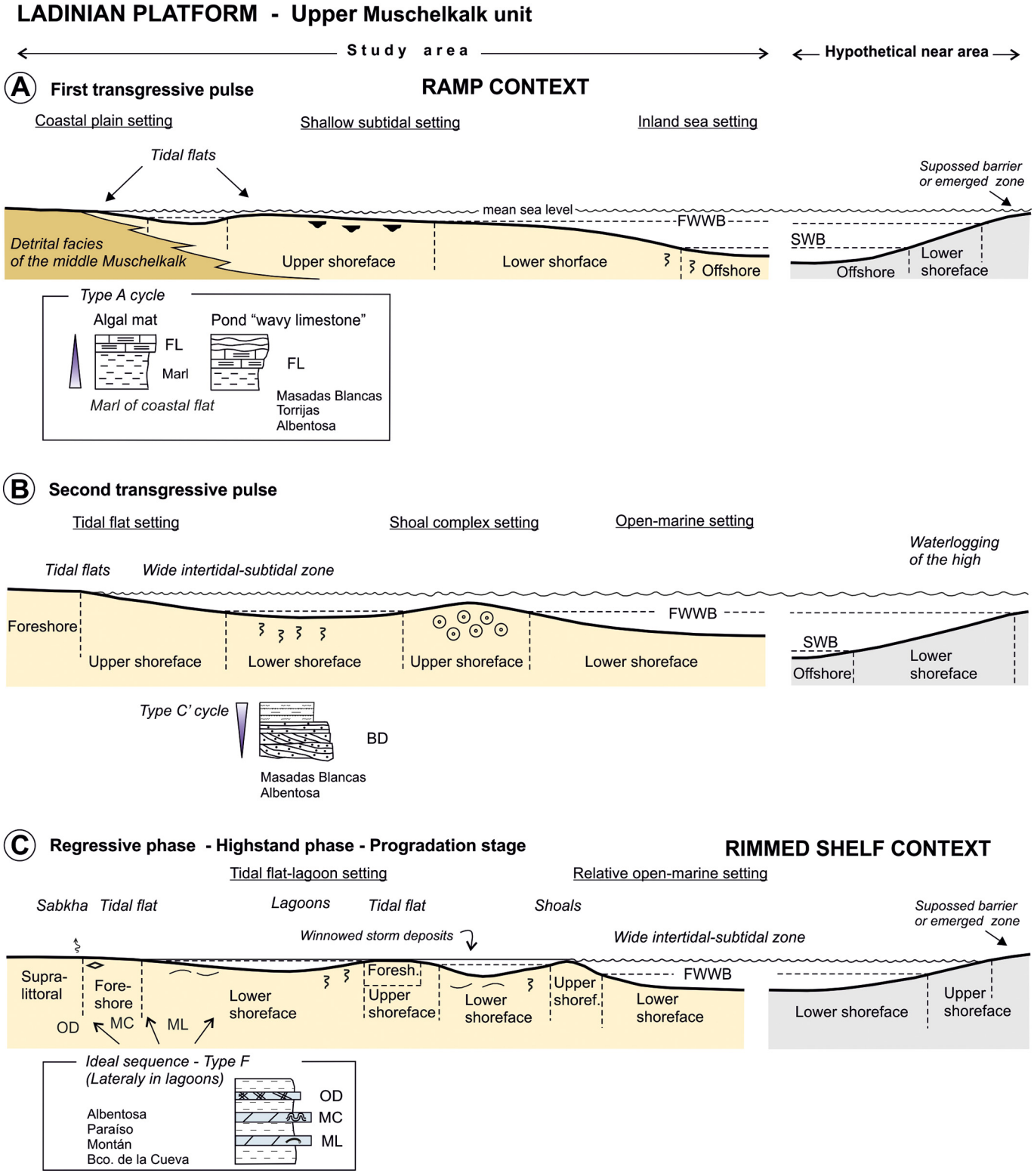

Fig. 17. Environments and platform model for the upper Muschelkalk unit (Ladinian). (A) Transgressive pulse in a ramp context. (B) Second transgressive pulse during the development of calcarenite shoals. (C) Regressive phase when shallow environments became established in a rimmed shelf context (upper carbonate-marl alternation).

phase is FA3 (lagoon), mainly consisting of marly limestones with bioturbation in the lower Muschelkalk unit and marly intercalations in the upper Muschelkalk unit. These two facies and their associated facies form a stacked progradational parasequence in the two Muschelkalk units. In general, the sedimentary environments of this first regressive phase were shallow, low energetic lagoons formed under restricted conditions. Shallowing-upward cycles are present in many lower Muschelkalk sections in the Alt Palància area. These cycles are formed at the base by 0.2 to 3 m thick marly limestone with bioturbations (LB facies) and at the top by massive carbonates containing bioclastic beds showing higher energy conditions (D cycle, Fig. 16C). A variable number of cycles are observed depending on the outcrops: 5 to 10 cycles within a 14–18 m thick interval in the Andilla–Bejís outcrop, and 4 to 8 cycles within a 12–34 m thick interval in the Montán–Espadà Ridge outcrops.

The stratigraphic interval in which these bioturbated-to-massive cycles occur shows a thickness between 4 m and some tens of meters.

9.4. Final regressive phase (late highstand)

Two different lithological assemblages, i.e. 'terminal carbonate complex' (FA1 and FA2) and 'upper carbonate-marl alternation' (FA2 and FA3), are recorded in the two Muschelkalk units during the final regressive phase. This phase is marked by a change in the characteristics of the deposits, especially in the areas of lower subsidence. In the lower Muschelkalk unit, the uppermost part is mainly (but not exclusively) made up of light gray to white, massive or laminated dolostones, and locally of stromatolite beds (MC facies). These carbonates, 20–35 m in thickness, are interpreted as sabkha deposits of the final regression. Evaporite molds, small calcite geodes (DDV facies), and thin-bedded breccias are frequent in these dolostones, as well as wave-undulated surfaces in some sections due to the effects of strong winds on the pond water. Also, a sedimentary cycle consisting of massive carbonates with calcite geodes and carbonates with laminations (E cycle, Fig. 16C) can be distinguished in this 'terminal carbonate complex' in the Molinar, Arteas, and Fuente la Reina sections (Figs. 4, 5). The top of this complex is marked by a white dolostone bed, 0.5 to 1.5 m thick, which is mainly comprised of stromatolite domes (MC facies). This characteristic top bed of the lower Muschelkalk unit records a sea-level fall linked to a lowstand stage (sequence boundary) at the end of this regressive phase and passes abruptly to the gray lutites of the middle Muschelkalk unit.

Despite the predominance of this complex at the top of the lower Muschelkalk unit, it is replaced by a thick carbonate-marl alternation in the Caudiel section. The carniolar and laminated facies (OD facies) become dominant at the top of the alternation forming shallowing upward sequences (Type F). This carbonate-marl alternation was deposited in restricted lagoons to peritidal settings (foreshore zone). It mainly represents the lateral facies variations of the different subenvironments that moved laterally. This indicates the instability of such shallow marine environments and that, over time, more supratidal deposits occur, first increasingly dominated by microbial carbonates and then by carniolar and/or evaporitic deposits. This is recorded in the different bed alternations that can be observed in the upper part of the Muschelkalk successions.

In the upper Muschelkalk unit, however, the final regressive phase is recorded mainly by an upper carbonate-marl alternation (ML and OD facies), which can locally reach 80 m in thickness (Montán section, Fig. 7). Only at the top of the Manzanera section is this carbonate-marl alternation replaced by a 'terminal carbonate complex' (Fig. 8) similar to the one present at the top of the lower Muschelkalk unit.

These features suggest lateral gradations between the two lithological assemblages in the two Muschelkalk units. The thick carbonate-marl alternation reflects lagoon (peritidal) areas, more subsident and influenced more by distal siliciclastic contributions from the continent. The alternations make gradual upwards transitions to evaporite environments, i.e. to the middle Muschelkalk facies in the case of the lower Muschelkalk unit, and Keuper facies in the case of the upper Muschelkalk unit. In contrast, the 'terminal carbonate complex' reflects less subsidence, with the greater development of supratidal and intertidal zones without siliciclastic material input, and shows a sharp change to overlying evaporite deposits.

10. Discussion

10.1. Platform model

The platform model proposed here for the lower and the upper Muschelkalk units of the study areas is shown in Figs. 18 and 19, respectively. We infer shallow environments for the two units during transgressive and regressive phases. The most widespread sediment types at the start and end of the units were lime mud and microbial tidal carbonates, whereas the most common deposits in the central parts were bioclastic calcarenites, bioturbated muds, and some oolitic deposits. No significantly deeper marine carbonates such as offshore or deep ramp deposits were identified, except occasionally, when some nodular offshore limestones are recognized. Accordingly, the proposed platform model is based on the idea that all these sediments correspond to the inner margin of a large, shallow epicontinental sea. In detail, however, a complex morphology characterized this shallow platform in which wave energy, currents and storm effects easily changed or were modified under the control of local and regional tectonics. The two stratigraphic units display shallowing-upward sequences in which storm deposits are sparse and seem to decrease upwards. The common presence of protected environments, mainly for the upper Muschelkalk unit, conditioned the sedimentation of the winnowed storm deposits that define the winnowed tempestite model (Pérez-López and Pérez-Valera, 2012).

For the two Muschelkalk units, the morphology of this epicontinental platform evolved from a shallow ramp (transgressive phases) to the final lagoon-peritidal-sabkha setting (regressive phases) initiating the change to evaporite facies. Under arid conditions and a low subsidence rate, this change was particularly rapid at the top of the lower Muschelkalk unit. Altogether, platform evolution was clearly controlled by local tectonics, and the study areas can be considered as one of the best-defined block-faulting sectors of the epicontinental platform in Eastern Iberia during Middle Triassic times. In the Alt Palància–Espadà Ridge area, the NW-SE oriented Espina–Espadà fault along with minor parallel faults exerted most structural control of Triassic sedimentation. For the Manzanera area, we infer the existence of a major basement fault oriented WSW–ENE driving Triassic sedimentation. This block-faulting sector of the epicontinental platform, however, was more affected by structural compartmentalization during the regressive phases than transgressive phases. In the case of the most common deposits at the top of the upper Muschelkalk unit (upper carbonate-marl alternation), this compartmentalization resulted in high environmental variability giving way to a complex mosaic of lagoons or inland seas. Subsidence then allowed for the stabilization of such environments in time but not space.

10.2. Comparisons with other areas and basins of Iberia

This section provides a brief comparison between the carbonate Muschelkalk units of the present study areas and those of other areas of the Iberian basin (Albarracín, Cuenca–València, Maestrat, and western sectors) as well as the Catalan basin and Prebetic–Subbetic domains of the Betic basin.

10.2.1. Lower Muschelkalk unit

The lower Muschelkalk unit (Fig. 20) is present in the central (Albarracín area) and eastern (Cuenca–València–Castelló) sectors of the Triassic Iberian basin, and in the Triassic Catalan and Ebro basins. The unit is absent in the Triassic Pyrenean, Basque–Cantabrian and Asturian basins, and in the Prebetic domain of the Betic basin (Fig. 1). The unit is known in the Iberian basin as Albarracín Fm, Landete Fm, and Oronet Fm (Fig. 3). Several reports have defined formal stratigraphic members of this unit (López-Gómez and Arche, 1992a; Calvet and Marzo, 1994; Garay Martín, 2001, 2005). The age of the unit is Anisian, mainly middle–late Anisian (Pelsonian–Illyrian). Its most outstanding characteristics and specific ages of the unit in the different sectors and basins are summarized in Supplementary data A.

For the lower Muschelkalk unit, a third-order depositional sequence is commonly assumed from the Catalan basin in the east to the Albarracín area of the Iberian basin in the west, where it thins out and disappears (Fig. 20). The complete evolution of this sequence was initially documented in the Iberian basin by López-Gómez and Arche (1992a, 1994) and Pérez-Arlucea and Rey (1994), and in the Catalan

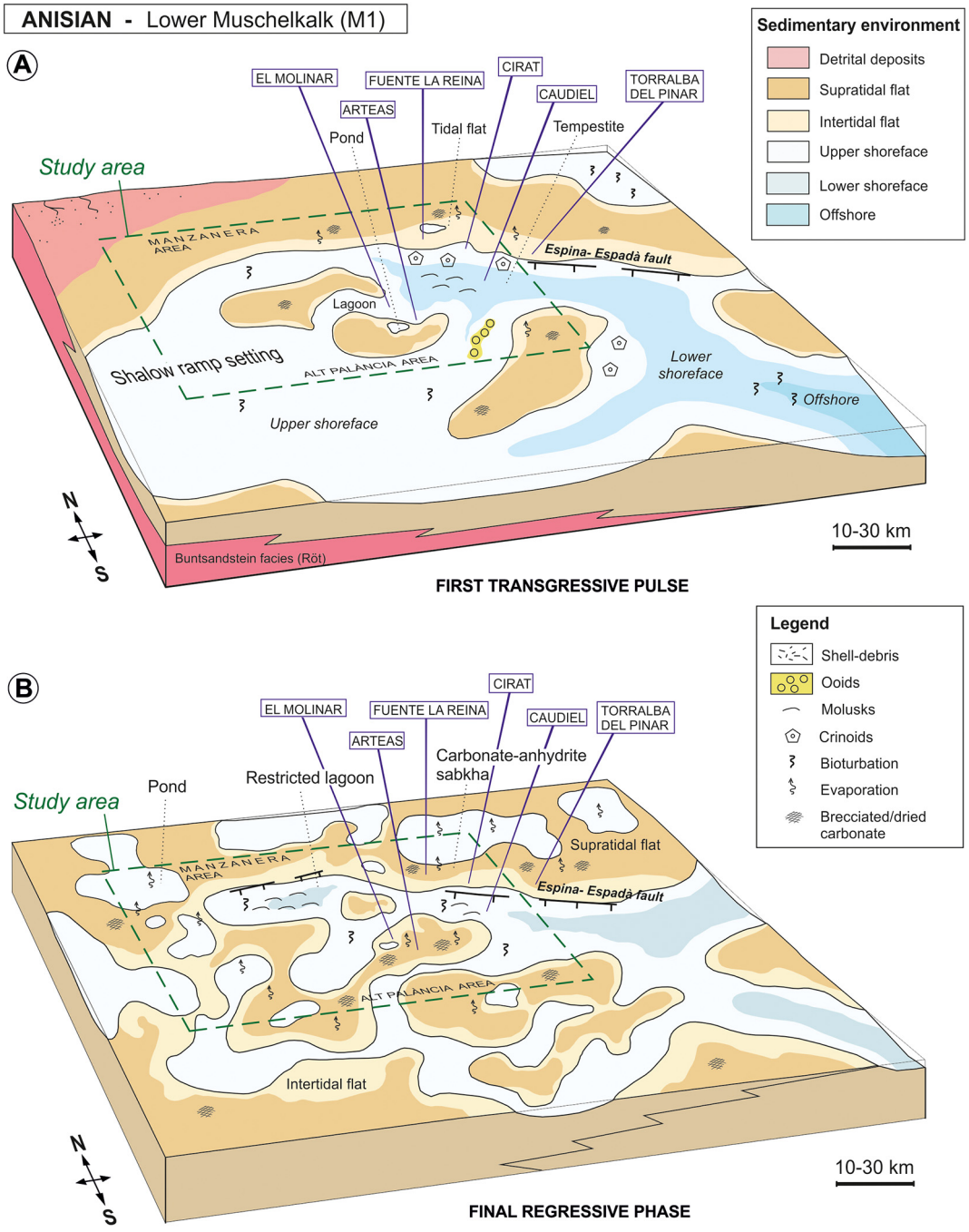

Fig. 18. Block diagrams of sedimentary environments in the lower Muschelkalk unit during the Anisian. (A) First transgressive pulse where new intertidal zones were established in a shallow ramp setting. The most abundant components of the sediments are crinoid fragments. The presence of ooids on the nearer shallower platform is inferred from oolitic tempestite microfacies. (B) During the final regressive phase, the most significant environment was a carbonate sabkha in which the sediments of the 'terminal carbonate complex' were deposited.

basin by Calvet et al. (1990) and Calvet and Marzo (1994), among other authors. Most of these studies make the assumption that the sub-units (members/units) of the transgressive phase (TST) begin with tidal flat settings and end with energetic shoals, whereas in the sub-units of the regressive phase (HST), the settings evolved from lagoons and restricted lagoons into final inter-supratidal environments with evidence of evaporite precipitates. The whole sequence mainly occurs in the shallow settings of the inner or inner-middle parts of a homoclinal ramp. The stratigraphic position of the maximum flooding surface is debatable in some sections, but usually it overlies the shoal tops of the transgressive phase. Most papers have described the higher order cyclicity characterizing the sub-units of this third-order sequence. Subsequent variations to this former literature interpretation are as follows: in the Albarracín sector, the sequence has been considered as strictly regressive (HST) by Pérez-Arlucea and Rey (1994) (Fig. 20, 4); in the Catalan basin, Calvet and Marzo (1994) distinguished two different pulses in the regressive trend (HST), i.e. early HST (Vilella Baixa unit) and late HST (Colldejou unit) (Fig. 20, 7); and in the northern part of the Iberian basin and also in the Catalan basin, Escudero-Mozo et al. (2015) divided the succession of the lower Muschelkalk unit into two trangressive–regressive sequences (Fig. 20, 5).

Further, in the depositional sequence of the lower Muschelkalk unit, some studies have identified the presence of significant features at regional or local scales such as unconformities, karstic horizons indicating

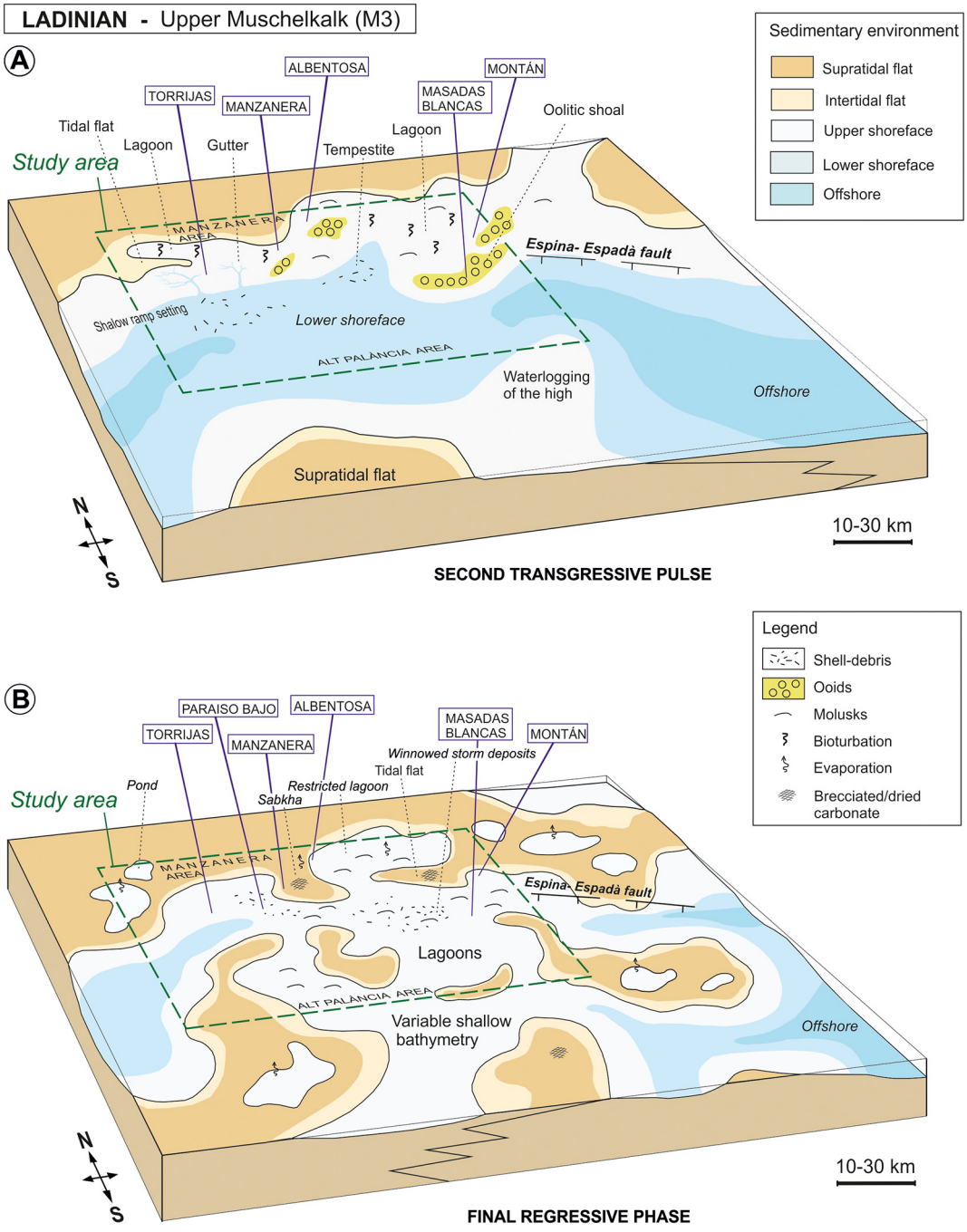

Fig. 19. Block diagrams of sedimentary environments in the upper Muschelkalk unit during the Ladinian. (A) Second transgressive pulse with oolitic shoals favored by increasing energy on the platform. (B) During the final regressive phase, lagoons developed under shallower conditions.

exposure events, and levels of faunal condensation linked to submarine hardgrounds or to prominent sea-level rises (drowning). In the Catalan basin, a regional unconformity was detected at the base of the youngest unit (Colldejou unit) by Calvet and Marzo (1994) (Fig. 20, 7). In the same basin, karst surfaces interrupting this sequence and associated Pb–Zn–Cu mineralizations (not indicated in Fig. 20) were described from the Prades sector in the SW to the Montseny-Llobregat sector in the NE (Andreu et al., 1987; Ramón and Calvet, 1987). Also in the Catalan basin, a fauna condensation horizon (*Paraceratites* level: ammonoids and conodonts), present at the top of the Olesa unit in the Montseny-Llobregat sector, was interpreted as the maximum flooding surface by Calvet and Marzo (1994) (Fig. 20, 7).

The boundary between the siliciclasic deposits of the Buntsandstein and the overlying tidal flat deposits of the lower Muschelkalk unit in the Iberian basin is marked by an unconformity involving high energy shoals and bars that separates the two units in the central (Albarracín) sector (Pérez-Arlucea and Rey, 1994). In contrast, in the eastern sectors of the basin, this transition is gradual (López-Gómez and Arche, 1992b; Ortí et al., 2020).

Our interpretation of the lower Muschelkalk unit in the Alt Palància of the Iberian basin is consistent with most stratigraphic and sedimentologic models proposed by the aforementioned papers, in particular, the shallow nature of the carbonate platform and the vertical evolution of its depositional sequence. In this area, the Anisian unit forms part of a single, third-order depositional sequence starting with siliciclastic tidal cycles of the Röt facies. The carbonate portion of the sequence was deposited on a very shallow epicontinental platform, showing various characteristics in the different

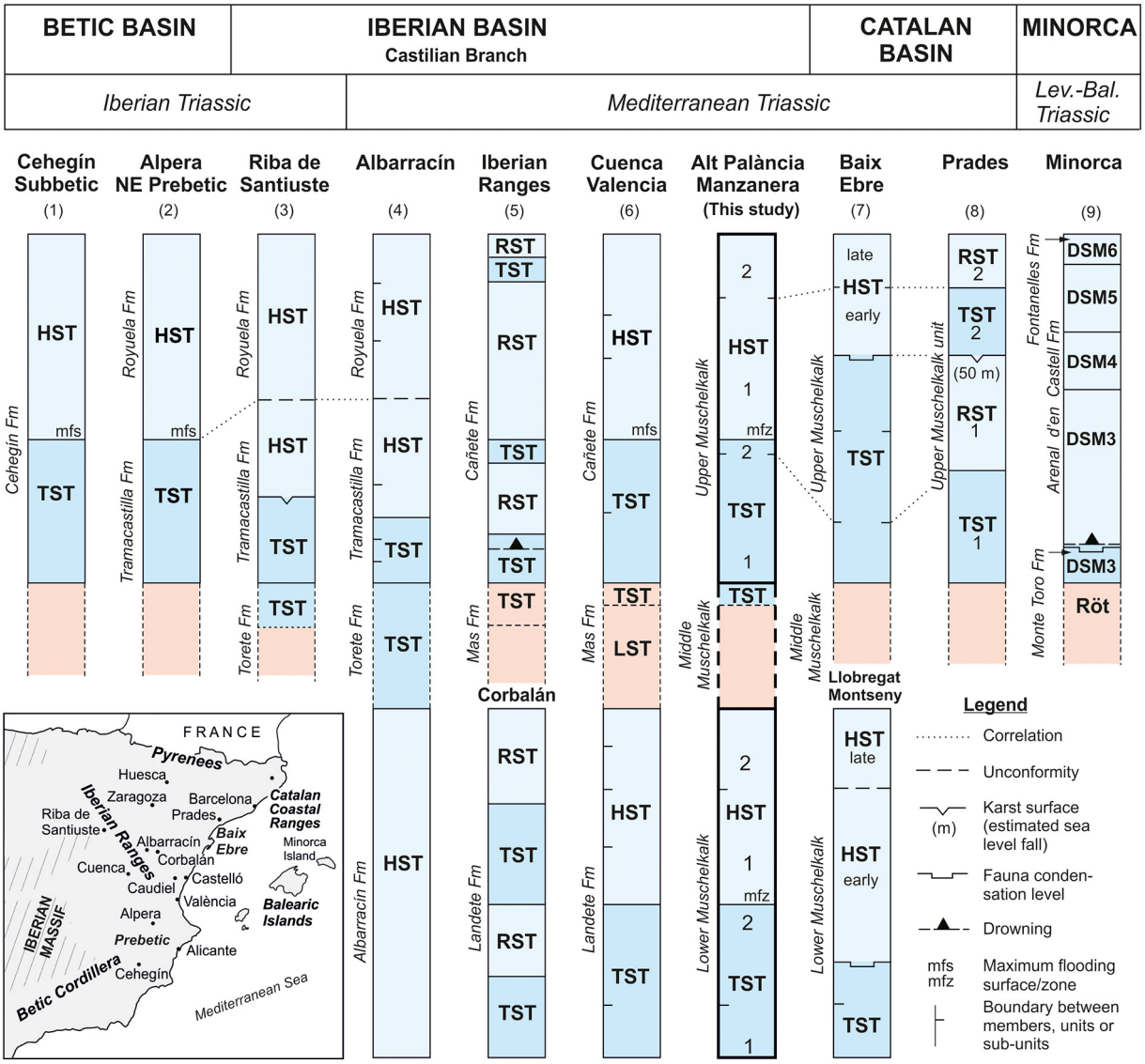

Fig. 20. Compilation of third-order depositional sequences in several Triassic basins and basin sectors of Eastern Iberia. References: (1) Pérez-Valera and Pérez-López (2008); (2) Sánchez-Moya et al. (2016); (3) García-Gil (1994); (4) Pérez-Arlucea and Rey (1994); (5) Escudero-Mozo et al. (2015); (6) López-Gómez and Arche (1994); (7) Calvet and Marzo (1994); (8) Mercedes-Martín et al. (2013a); (9) Escudero-Mozo et al. (2015). Sequence stratigraphy: LST: Lowstand System Tracts; TST: Transgressive System Tracts; HST: Highstand System Tracts. Transgressive/Regressive cycles: TST/RST. Depositional Sequence: DSM. Members/units/sub-units in the stratigraphic formations from base to top: (4) *Tramacastilla Fm*: Gea, Rincón, Chequilla, El Cuervo and El Castellar members. *Royuela Fm*: Libros Marls, Libros Limestones, and Villel members. (6) *Landete Fm*: Serra, San Martín, Olocau, Peña Rubia and Beaumud members. *Cañete Fm*: Gorgocil, Henarejos, Huélamo, Valacloche and Moya members. (This study) *lower and upper Muschelkalk units*: lower carbonate-marl alternation, carbonate sub-unit, upper carbonate-marl alternation. (7) *Lower Muschelkalk unit*: El Brull, Olesa, Vilella Baixa and Colldejou units. *Upper Muschelkalk unit*: Rojals, Benifallet, Rasquera, Tivissa and Capafons units.

sections studied, which were clearly controlled by the Espina–Espadà fault.

This study also highlights the following features of the lower Muschelkalk unit: (i) two pulses operating during transgressive (TST) and two phases during regressive (HST) sequences; (ii) depositional continuity from the siliciclastic-marl cycles of the Röt facies to the carbonate-marl cycles characterizing the mixed tidal flat at the base of the sequence (lower carbonate-marl alternation); (iii) paleogeographic variability in facies and environments affecting the intermediate carbonate sub-unit and preventing clear lateral correlations between the various carbonate intervals (Fig. 15); the maximum flooding zone is located in different stratigraphic intervals on both sides of the Espina–Espadà fault; and (iv) the possibility of finding at the top of the sequence, lateral gradations between predominant carbonate tidal flat ('terminal carbonate complex') and mixed tidal flat deposits (upper carbonate-marl alternation). In summary, the deposition of the lower Muschelkalk unit occurred on a fault-controlled, subsident (thicknesses up to >100 m) platform which was particularly shallow and productive, and relatively little affected by the most important events (regional unconformities, karst surfaces, faunal condensation levels) recorded in other sectors of the Iberian basin or adjacent basins.

10.2.2. Upper Muschelkalk unit

The upper Muschelkalk unit was deposited in Iberia during the second marine transgression of the Middle Triassic linked to the opening of the Neotethys Sea (Escudero-Mozo et al., 2015). This transgression covered all of Eastern Iberia and its deposits are present in all Triassic basins including the Subbetic and Prebetic domains of the Betic basin and Balearic Islands (Figs. 1, 20). In the Iberian basin, this unit is known as the assemblage of the Tramacastilla Fm and Royuela Fm in the western-central sector, as the Cañete Fm in the central and eastern sectors, and as the assemblage of the Cirat Fm and Pina de Montalgao Fm in the Calderona–Espadà ridges of the Valencian sector. In the Betic basin, it is known in the Prebetic domain as the assemblage of the

Tramacastilla Fm and Royuela Fm (Sopeña et al., 1988) and as the Siles Fm (Pérez-Valera and Pérez-López, 2008), and in the Subbetic domain as the Cehegín Fm (Pérez-Valera and Pérez-López, 2008). On Menorca Island, it is known as the assemblage of the Monte Toro Fm, Arenal d'en Castell Fm and Fontanlles Fm (Fig. 20). The most outstanding characteristics of this unit including its stratigraphic members distinguished by several authors are summarized in Supplementary data B.

The age assigned to this unit in the Iberian basin, according to the authors, is Ladinian or late Anisian (Illyrian)–Ladinian. In its most representative section of the Iberian basin (Cañete Fm; ~98 m thick), its age is Illyrian in the lower part (~17 m thick), Fassanian in the central part (~61 m thick) and Longobardian in the upper part (~20 m thick) (Escudero-Mozo et al., 2019; Fig. 3.35). In the Alt Palància area of this study, Ortí et al. (2020) confirmed the general assignment of the unit to the Ladinian (Fassanian stage more clearly documented). In the Catalan basin, its age is upper Ladinian (Longobardian)–earliest Carnian ('Cordevolian') (García-Ávila et al., 2020). On Minorca, the unit has been assigned to the late Anisian (Illyrian)-to-early Carnian (Escudero-Mozo et al., 2014, 2015).

Several interpretations of depositional sequences have been proposed for the upper Muschelkalk unit in the different Triassic basins of Iberia (Fig. 20). A single third-order depositional sequence is commonly assumed for this unit, from the Catalan basin in the east to the Riba de Santiuste area of the Iberian basin in the west. In the Catalan basin, one depositional sequence was recognized by Calvet and Marzo (1994) (Fig. 20, 7), two depositional sequences were identified by Calvet and Tucker (1995), and two transgressive–regressive sequences (T–R) were documented by Mercedes-Martín et al. (2013a). Escudero-Mozo et al. (2015) described two or three transgressive–regressive sequences (T–R) in the Catalan and Iberian basins, and three or four in Minorca in the formations equivalent to the upper Muschelkalk unit (Monte Toro Fm, Arenal d'en Castell Fm and Fontanelles Fm) (Fig. 20).

Carbonate facies deeper than those observed in the lower Muschelkalk unit have been interpreted for the upper Muschelkalk unit in the Triassic basins of Iberia, in particular in the middle part of the sequences (Supplementary data B). In the Albarracín sector of the Iberian basin, deep outer ramp settings were assigned to the Chequilla and Rincón members by Pérez-Arlucea and Rey (1994), and environments of inner, middle and outer ramp were described for the entire basin by Escudero-Mozo et al. (2015). In the Catalan basin, deep ramp deposits (Rasquera unit) and deep to shallow ramp deposits (Tivissa unit) were interpreted by Calvet and Marzo (1994). Also in the Catalan basin, environments of deep outer ramp (towards the SE of the basin), mid-ramp (central part) and inner ramp (towards the NE of the basin) were interpreted by Mercedes-Martín et al. (2013a). In the Betic basin, the upper Muschelkalk carbonates (Cehegín Fm and Siles Fm) show characteristics of a shallow epicontinental platform. Most sediments were deposited in a coastal setting, and other marine sediments were scattered across a varied mosaic of lagoons and restricted inland seas (Pérez-Valera and Pérez-López, 2008; Pérez-López et al., 2011). Very few deep deposits were identified in the two areas of the present study. The upper Muschelkalk sediments in the lower half of the carbonate sub-unit indicate ramp settings with partial communication with the open sea. All these interpretations of sedimentary environments confirm the complexity of the Triassic epicontinental platform highlighted in this study, mainly due to the generally low bathymetry of these marine environments and the important role of local tectonics.

Two of the most significant events recorded in the upper Muschelkalk successions of the Triassic basins in Eastern Iberia (Fig. 20) were not identified in the study area. One event refers to the erosive karst surface that separates the two transgressive–regressive sequences in the Catalan basin. This surface has been interpreted as a basin scale sea-level fall of over 50 m by Mercedes-Martín et al. (2013a, 2013b). The other event is a rapid sea-level rise recorded at the Anisian–Ladinian transition at the top of the Monte Toro Fm in Minorca (Escudero-Mozo et al., 2014, 2015). This marine rise resulted in local drowning, carbonate deposition in middle–outer ramp settings, and the accumulation of Daonella shells and ammonoids. Escudero-Mozo et al. (2014, 2015) correlated this event with the condensation fauna level described by Calvet and Marzo (1994) at the base of the Rasquera unit in the Catalan basin (Fig. 20), and extended this abrupt sea-level rise to all sectors of the Iberian basin.

The lack of the two former events indicated by our observations in the Alt Palància and Manzanera areas possibly reflects the shallow-water nature and the paleogeographic features of the carbonate platform during deposition of the upper Muschelkalk unit. Moreover, several characteristics such as the high variability of settings throughout the middle carbonate sub-units, the presence of carbonate marl alternations at the base and top of the sequences, and lateral gradations between these alternations and the terminal carbonate complexes do not support the use of formal member names. As a result, this terminology seems to have been abandoned in recent papers addressing the carbonate Muschelkalk units of Eastern Iberia (Mercedes-Martín et al., 2013a; Sánchez-Moya et al., 2016; Escudero-Mozo et al., 2015, 2016).

10.3. Comparison with the Muschelkalk of the Germanic Basin

The similarity of facies and environments in the two carbonate Muschelkalk successions of Eastern Iberia was highlighted in the former sections, although there are some differences between the two successions. One notable difference is that the upper Muschelkalk deposits become more marine and reflect higher subsidence rates, as indicated by the section's thickness, and the increased presence of mollusk fossils, ooids, and storm beds. Something similar occurs in the Triassic of the Germanic Basin. Besides presenting mainly fine-grained carbonate facies with bioclastic sandbanks and tempestites, the upper Muschelkalk deposits of the Germanic Basin are also more marine (e.g., Aigner and Bachmann, 1992). The evolution of the Germanic Basin was controlled by tectonics in the Tethys rift belt (Szulc, 1999) as can be observed in the different basins of Eastern Iberia. According to Szulc (2000), these variations in stratigraphic units are more frequent in the upper Muschelkalk. In fact, the sequences defined in the western sector of the German Basin show marked individual characteristics suggesting the strong influence of local tectonic controls. Although deposition was controlled by global sea-level changes, these eustatic changes were modified by local tectonics.

Asymmetric transgression–regression cycles are observed in the two basins (Fig. 21), although with different facies evolutions. Facies distribution are markedly diachronous in the Germanic Basin and in the basins of Eastern Iberia. At the end of these Muschelkalk carbonate sequences, the uplift of the basins led to an increase in clastic sediments during the deposition of the Keuper facies, but this change occurred more rapid and earlier in the Germanic Basin (Szulc, 2000; Feist-Burkhardt et al., 2008).

The studied carbonates of the lower Muschelkalk in Eastern Iberia show depositional conditions similar to those of the lower Muschelkalk of northwestern Germany, which was affected by restricted circulation, closer to an evaporite basin, where sabkha facies developed locally (Feist-Burkhardt et al., 2008). However, scarce sulfate is associated with the sabkha carbonates in Eastern Iberia. The other fully marine facies (Terebratelbanke) observed towards southeastern Germany in the lower Muschelkalk are not present in the studied outcrops of Eastern Iberia. The most similar facies of lower Muschelkalk would be the marly limestones of the Wellenkalk formation, although carbonate sabkha and lagoon deposits predominated in Eastern Iberia (Fig. 21).

As in the Germanic basin, the Upper Muschelkalk carbonates studied by us in Eastern Iberia were deposited during the Ladinian transgression. In this area, however, a high-energy ramp was not established as is the case in the Germanic Basin (Trochitenkalk/Trochiten-Schichten). The sediments of the Germanic Basin comprise mainly bioclastic and

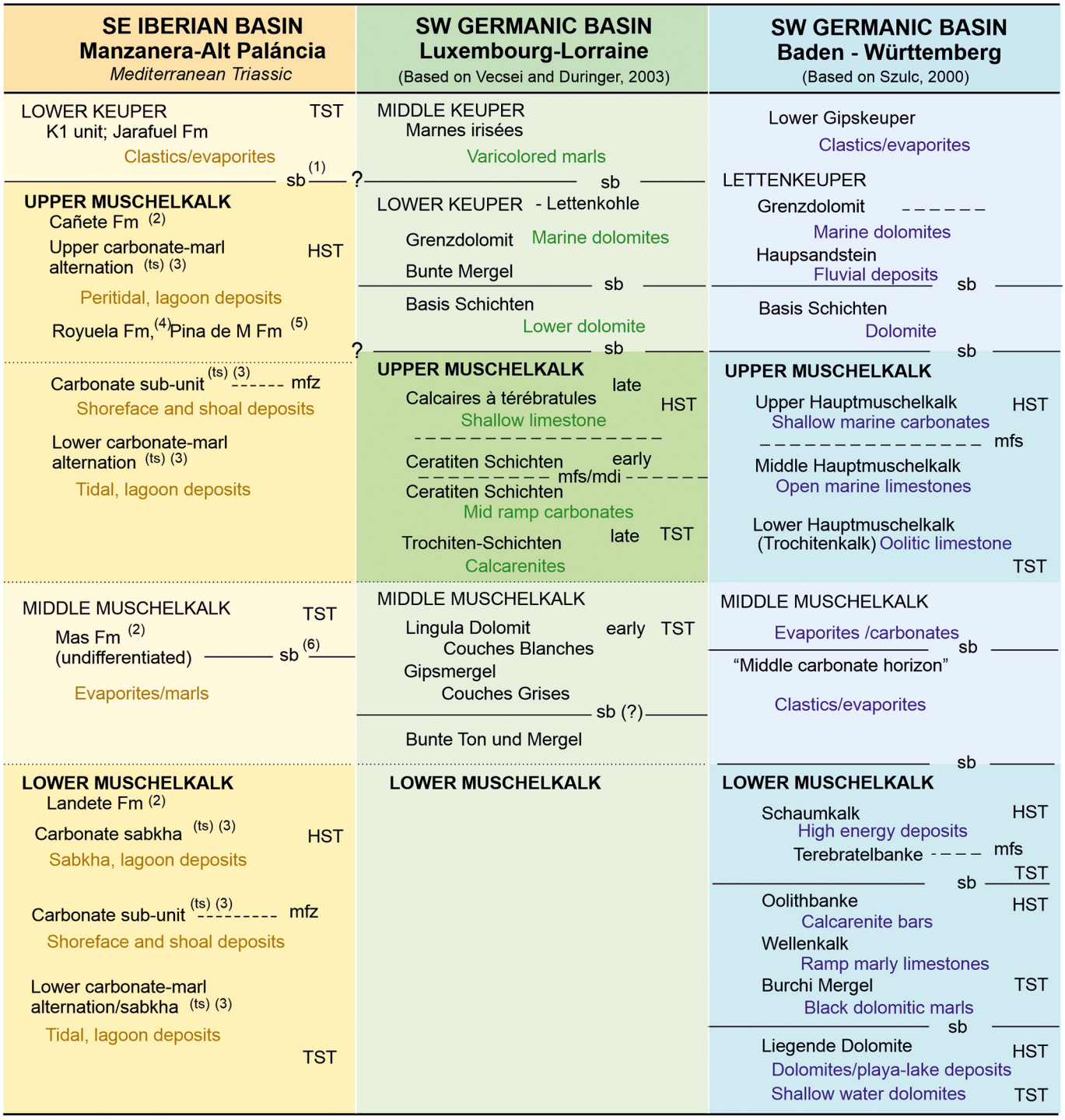

Fig. 21. Comparison of stratigraphic units and third-order depositional sequences in the Middle Muschelkalk to Middle Keuper interval in the SW Germanic and the SE sector of the Iberian basins. The LST, which is not indicated in the figure, is represented by erosive or karst surfaces or by thin evaporite or carbonate beds. Symbols and references in the SE Iberian Basin: (*) Mediterranean Triassic; (ts) this study; (1) Ortí et al., 2017; (2) López-Gómez et al., 1998; (3) Ortí et al., 2020; (4) Sánchez-Moya et al., 2016; (5) Garay Martín, 2005; (6) Escudero-Mozo et al., 2015.

oolitic sediments (TST) , on top of which, deep carbonate ramp sediments were deposited (Middle Hauptmuschelkalk/Ceratiten Schichten). In the studied sectors of Eastern Iberia, however, the ramp was sheltered by some barrier or emergent zone located much farther to the east. The first upper Muschelkalk sediments are of low energy conditions. Bioclastic or oolitic sediments, which in the studied sectors are recorded by brown dolostones, do not appear until the second transgressive phase of the Ladinian. Finally, during the highstand stage, the shallow marine deposits prograded over the normal marine carbonates in the Germanic Basin (Aigner, 1985), although only lower energy conditions reflect the sediments in Eastern Iberia (Upper carbonate-marl alternation). Lithofacies distributions and fauna assemblages in the Germanic Basin were conditioned in their communication with the Tethys Ocean through the SW sector or the western Gate (Szulc, 2000).

In the Lorrain region of the SW Germanic Basin, Vecsei and Duringer (2003) described a classic model of carbonate platform in a transect from the margin (western Luxembourg) to the depocenter (northern France). The model is characterized by an environment belt grading from shore to deep shelf. This model is clearly different from the mosaic

model of shallow settings here deduced in the studied area of Eastern Iberia. It should be noticed that the Lower Keuper in the SW Germanic Basin occupies the same stratigraphic position as the upper carbonate-marl alternation (Royuela Fm) of Ladinian age in the Iberian basin (Fig. 21).

The maximum flood surface in the Germanic Basin can be located between different lithofacies. These lithofacies are more marine towards the center of the basin, while towards the margin, this surface separates calcarenite sediments or bar deposits below from lagoon deposits above (Vecsei and Duringer, 2003). In most of the studied sections in Eastern Iberia, the maximum flood surface represented by the maximum flooding zone is situated in the brown dolosparites. This lithofacies records the higher energy deposits that developed when the sea level rose and overtopped the inferred barriers located further east of the study area (Figs. 16, 17).

The stratigraphic sequences defined in the Germanic Basin are based on the presence of major discontinuities and significant fossil variation allowing for the establishment of maximum flood surfaces. In contrast, in the present study area, fossils are rather scarce and no precise marked beds were identified as possible sequence boundaries.

Two transgression–regression sequences can be identified for the lower and the upper Muschelkalk units in the studied area of Eastern Iberia. In the SW Germanic Basin, however, two transgression–regression sequences have been defined for the lower Muschelkalk, and only one for the upper Muschelkalk.

11. Conclusions

In the study areas of Eastern Iberia, two marine flooding episodes of the Middle Triassic caused the extensive deposition of carbonates in the lower and upper Muschelkalk units on a block-controlled, shallow, epicontinental platform. Based on paleontological data available in the literature (palynology and ammonoids data), the lower Muschelkalk unit is assigned to the Anisian and the upper Muschelkalk unit to the Ladinian. In outcrops showing signatures of severe tectonism, identification through sulfate isotopy of the clayey-evaporite facies bounding the carbonates (Keuper and middle Muschelkalk) helped us to distinguish the two carbonate Muschelkalk units.

Each of the carbonate Muschelkalk units forms part of a third-order depositional sequence and can be subdivided into two transgressive and two regressive phases. Both sequences show similar vertical arrangements of stratigraphic sub-units, and appear uninterrupted by unconformities.

The two Muschelkalk sequences start with a (lower) carbonate-marl alternation, which was deposited in mixed tidal flat-to-lagoon settings. In the middle part of the sequences (carbonate sub-unit), the carbonate character prevails and facies associations suggest great variability occurring in relatively shallow environments. The change from transgressive to regressive trends occurs in this middle part. The tops of the sequences show two coeval lithologic assemblages, i.e. the 'terminal carbonate complex' formed in tidal flats and sabkhas, and the 'carbonate-marl alternation' formed in carbonate tidal flat-to-lagoon settings. The 'terminal carbonate complex' predominates in the lower Muschelkalk unit, but locally it grades laterally to the carbonate-marl alternation. The 'carbonate-marl alternation' is predominant in the upper Muschelkalk unit, but locally it also grades laterally to the terminal carbonate complex.

In the two carbonate sequences, the presence of carbonate-marl alternations underlying and overlying the massive carbonates of the middle part should be highlighted. In the study outcrops, these alternations occur mainly in fault-controlled areas with continuous subsidence. This gave rise to lithologic gradations instead of sharp contacts between the middle carbonate sub-units and the clayey-evaporite deposits of the Röt, middle Muschelkalk and Keuper facies.

The two carbonate Muschelkalk sequences suggest a complex morphology of the epicontinental platform which evolved from not very high-energy ramp-like profiles (transgressive phases, TST) to a low energy rimmed shelf terminating in tidal/lagoon settings (regressive phases, HST). The facies associations, however, suggest depositional settings that were slightly deeper for the upper Muschelkalk unit than for the lower Muschelkalk unit.

In the Alt Palància area, sedimentation during the Middle Triassic controlled by the major Espina–Espadà fault was confirmed here. In the Manzanera area, similar control by a (non outcropping) basement fracture is assumed.

By comparing our Muschelkalk sequences with those known in other basins of Eastern Iberia, here we highlight some of the most relevant characteristics of the carbonate accumulation in the study areas such as shallow-water settings, mosaic facies patterns in the middle of the sequences, and absence of significant discontinuities interrupting sedimentation. In comparison to the Middle Triassic of the SW Germanic Basin, several deposits with similar facies, typical of an epicontinental platform, were here identified, although the facies exhibit shallower water features, with less siliciclastics, and the definition of facies belts within the platform model is uncertain.

Declaration of competing interest

The authors declare no known competing financial interests or personal relationships that could have influenced the work reported in this paper.

Acknowledgments

This study was supported by Projects PID2019-104625RB-100 and PGC2018-098272-B-I00 (Secretaría de Estado de I+D+I, Spain), B-RNM-072-UGR18 (FEDER Andalucía), P18-RT-4074, RNM-208 (Junta de Andalucía), and 2017SGR-824 (SEDIMENTARY GEOLOGY) of the Catalan Government (Departament d'Innovació, Unversitats i Empresa). The authors thank Annette Götz (Landesamt für Bergbau, Energie und Geologie, Geozentrum Hannover) for her comments on micropaleontology identification and suggestions regarding the writing of the manuscript, Policarp Garay Martín for supplying relevant geological documentation for the Alt Palància area, Eusebio García for valuable field assistance, Joan Guimerà, Ramón Mercedes, Ramón Salas, Juan Diego Martín Martín (Universitat de Barcelona) for fruitful discussions on the Triassic of the northern Valencian Country and Catalunya, and Fotini Pomoni-Papaioannou and an anonymous reviewer for significantly improving the manuscript.

Appendix A. Supplementary data

Supplementary data to this article can be found online at https://doi.org/10.1016/j.sedgeo.2021.105904.

References

Adams, A., Diamond, L.W., 2019. Facies and depositional environments of the Upper Muschelkalk (Schinznach Formation, Middle Triassic) in northern Switzerland. Swiss Journal of Geosciences 112, 357–381. https://doi.org/10.1007/s00015-019-00340-7.

Aigner, T., 1985. Storm Depositional Systems. Lecture Notes in Earth Sciences. Springer Verlag, Berlin (174 pp.).

Aigner, T., Bachmann, G., 1992. Sequence-stratigraphic framework o f the German Triassic. Sedimentary Geology 80, 115–135.

Alonso-Azcárate, J., Bottrell, S.H., Mas, J.R., 2006. Synsedimentary versus metamorphic control of S, O and Sr isotopic compositions in gypsum evaporites from the Cameros Basin, Spain. Chemical Geology 234, 46–57.

Andreu, A., Calvet, F., Font, X., Viladevall, M., 1987. Las mineralizaciones de Pb-Zn-Ba en el Muschelkalk inferior de los Catalánides. Cuadernos de Geología Ibérica 11, 779–795 (in Spanish with English abstract).

Arche, A., López-Gómez, J., 1996. Origin of the Permian-Triassic Iberian Basin, central–eastern Spain. Tectonophysics 266, 443–464.

Bertram, G.T., Bally, A.W., 2012. Seismic and sequence stratigraphic analysis. In: Roberts, D.G. (Ed.), Regional Geology and Tectonics: Priciples of Geologic Analysis. Elsevier, pp. 345–376.

Bodzioch, A., Kwiatkowski, S., 1992. Sedimentation and early diagenesis of Cavernous Limestone (Roet) of Gogolin, Silesian - Kraków Region. Annales. Societatis Geologorum Poloniae 62, 223–254.
Calvet, F., Marzo, M., 1994. El Triásico de las Cordilleras Costero Catalanas: estratigrafía, sedimentología, y análisis secuencial. III Coloquio de Estratigrafía y Paleogeografía del Pérmico y Triásico España, Cuenca. Excursion Guide-book. p. 53 (in Spanish).
Calvet, F., Tucker, M.E., 1995. Mud-mounds with reefal caps in the Upper Muschelkalk (Triassic), eastern Spain. In: Monty, C.L.V., Bosence, D.B., Bridges, P., Pratt, B. (Eds.), Mud Mounds: Origin and Evolution. International Association of Sedimentologists, Special Publication 23. Blackwell Scientific Publications, Oxford, pp. 311–333.
Calvet, F., Tucker, M.E., Henton, J.M., 1990. Middle Triassic carbonate ramp systems in the Catalan Basin, northeast Spain: facies, systems tracts, sequences and controls. In: Tucker, M.E., Wilson, J.L., Crevello, P.D., Sarg, J.R., Read, J.F. (Eds.), Carbonate Platforms, Facies, Sequences and Evolution. Special Publications International Association of Sedimentologists vol. 9. Blackwell Scientific Publications, Oxford, pp. 79–108.
Castillo, E., 1980. Síntesis hidrogeológica del Sistema n° 56. Sierra de Espadán y Plana de Castellón. Instituro Geologico y Minero de España (IGME), Estudios de Gestión y Conservación de Acuíferos, t. 4: Actualización de balances, reevaluación de recursos y reservas, perfeccionamiento del grado de conocimiento, Anejo D, December 1980. p. 111 (in Spanish).
Cattaneo, A., Steel, R.J., 2003. Transgressive deposits: a review of their variability. Earth-Science Reviews 62, 187–228.
Chatalov, A., 2013. A Triassic homoclinal ramp from the Western Tethyan realm, Western Balkanides, Bulgaria: integrated insight with special emphasis on the Anisian outer to inner ramp facies transition. Palaeogeography, Palaeoclimatology, Palaeoecology 386, 34–58. https://doi.org/10.1016/j.palaeo.2013.04.028.
Chatalov, A., 2017. Anachronistic and unusual carbonate facies in uppermost Lower Triassic rocks of the western Balkanides, Bulgaria. Facies 63, 24. https://doi.org/10.1007/s10347-017-0505-0.
Costamagna, L.G., Barca, S., 2002. The "Germanic" Triassic of Sardinia (Italy): a stratigraphic, depositional and paleogeographic review. Rivista Italiana di Paleontologia e Stratigrafia 108, 67–100.
Delgado, F., 1977. Primary textures in dolostones and recristallized limestones: a technique for their microscopic study. Journal of Seminentary Petrology 47 (3), 1339–1341.
Diedrich, C.G., 2009. Palaeogeographic evolution of the marine Middle Triassic marine Germanic Basinchangements – with emphasis on the carbonate tidal flat and shallow marinehabitats of reptiles in Central Pangaea. Global and Planetary Change 65, 27–55.
Dunham, R.J., 1962. Classification of carbonate rocks according to depositional texture. American Association of Petroleum Geologists Memoir 1, 108–121.
Duringer, P., Vecsei, A., 1998. Middle Triassic shallow-water limestones from the Upper Muschelkalk of eastern France: the origin and depositional environment of some early Mesozoic fine-grained limestones. Sedimentary Geology 121, 57–70.
Embry, A., Klovan, J.E., 1971. A late Devonian reef tract on northeastern Banks Island, Northwest Territories. Bulletin of Canadian Petrolem Geology 19, 730–781.
Escudero-Mozo, M.J., 2015. Las plataformas carbonáticas del Triásico (facies Muschelkalk) del este de Iberia y Menorca: Implicaciones en la evolución paleogeográfica del oeste del Tethys. Universidad Complutense de Madrid (Ph.D. thesis, 345 pp., in Spanish with English abstract).
Escudero-Mozo, M.J., Márquez, L., López-Gómez, J., Martín-Chivelet, J., 2012. Foraminíferos Anisienses en la Fm. Landete (facies Muschelkalk): implicacions bioestratigráficas para la primera transgresión mesozoica en el SE de la Cordillera Ibérica. Geogaceta 51, 31–34 (in Spanish with English abstract).
Escudero-Mozo, M.J., Márquez-Aliaga, A., Goy, A., Martín-Chivelet, J., López-Gómez, J., Márquez, L., Arche, A., Plasencia, P., Pla, C., Sánchez-Fernández, D., 2015. Middle Triassic carbonate platforms in eastern Iberia: evolution of their fauna and palaeogeographic significance in the western Tethys. Palaeogeography, Palaeoclimatology, Palaeoecology 417, 236–260.
Escudero-Mozo, M.J., Martín-Chivelet, J., Goy, A., López-Gómez, J., 2014. Middle–Upper Triassic carbonate platforms in Minorca (Balearic islands): implications for Western Tethys correlations. Sedimentary Geology 310, 41–58.
Escudero-Mozo, M.J., Martín-Chivelet, J., López-Gómez, J., Arche, A., Márquez-Aliaga, A., Goy, A., Márquez, L., Plasencia, P., Sánchez-Fernández, D., 2019. The Middle Triassic carbonate ramps (Muschelklak) in the Iberian Basin. In: Quesada, C., Oliveira, J.T. (Eds.), The Geology of Iberia: A Geodynamic Approach. Volume 3: The Alpine Cycle. Springer, Heidelberg, pp. 74–76.
Escudero-Mozo, M.J., Pérez-Valera, J.A., Hirsch, F., Márquez, L., Márquez-Aliaga, A., Pérez-López, A., Pérez-Valera, F., Plasencia, P., 2016. In: Meléndez, G., Núñez, A., y Tomás, M. (Eds.), Actas de las XXXII Jornadas de la Sociedad Española de Paleontología. Cuadernos del Museo Geominero, n° 20. Instituto Geológico y Minero de España, Madrid, pp. 53–60 (in Spanish).
Feist-Burkhardt, S., Götz, A.E., Szulc, J., Borkhataria, R., Geluk, M., Haas, J., Hornung, J., Jordan, P., Kempf, O., Michalík, J., Nawrocki, J., Reinhardt, L., Ricken, W., Röhling, H.-G., Rüffer, T., Török, Á., Zühlke, R., 2008. Triassic. In: McCann, T. (Ed.), The Geology of Central Europe. vol. 2. Geological Society London, pp. 749–821 (coordinators).
Flügel, E., 2004. Microfacies of Carbonate Rocks. Springer, Berlin Heidelberg, New York.
Garay Martín, P., 2001. El dominio triásico Espadán-Calderona. Contribución a su conocimiento geológico e hidrogeológico. Universidad de València (Ph.D. thesis, 692 pp., in Spanish).
Garay Martín, P., 2005. Unidades litoestratigráficas del Triásico Medio en el dominio Espadán-Calderona (provincias de Castellón y Valencia). Geo-Temas 8, 159–162 (in Spanish with English abstract).
García-Ávila, M., Mercedes-Martín, R., Juncal, M.A., Diez, J.B., 2020. New palynological data in Muschelkalk fàcies of the Catalan Coastal Ranges (NE of the Iberian Peninsula). Comptes Rendus Géoscience-Sciences de la Planète 352, 443–454. https://doi.org/10.5802/crgeos.8.
García-Gil, S., 1994. El Triásico de la región de Riba de Santiuste-Arcos de Jalón. III Coloquio de Estratigrafía y Paleogeografía del Pérmico y Triásico España, Cuenca. Excursion Guide-book (52 pp., in Spanish).
Gingras, M.K., Bann, K.L., MacEachern, J.A., Pemberton, S.G., 2009. A conceptual framework for the application of trace fossils. In: MacEachern, J.A., Bann, K.L., Gingras, M.K., Pemberton, S.G. (Eds.), Applied Ichnology. Short Course Notes vol. 52. Society for Sedimentary Geology, Tulsa, pp. 1–26.
Goy, A., 1995. Ammonoideos del Triásico Medio de España: Bioestratigrafía y Correlaciones. Cuadernos de Geología Ibérica 19, 21–60 (in Spanish with English abstract).
Handford, C.R., Loucks, R.G., 1993. Carbonate depositional sequences and systems tracts; responses of carbonate platforms to relative sea-level changes. In: Loucks, R.G., Sarg, J.F. (Eds.), Carbonate Sequence Stratigraphy; Recent Developments and Applications. American Association of Petroleum Geologists Memoir vol. 57, pp. 3–41.
Hinkelbein, K., 1969. El Triásico y el Jurásico de los alrededores de Albarracín. Teruel 41, 35–75 (in Spanish).
IGME, 1974a. Memoria y mapa geológico de España a escala 1:50.000. Hoja de Manzanera (614). Ministerio de Industria, Instituto Geologico y Minero de España (IGME), Madrid.
IGME, 1974b. Memoria y mapa geológico de España a escala 1:50.000. Hoja de Segorbe (640). Ministerio de Industria, Instituto Geologico y Minero de España (IGME), Madrid.
IGME, 1975. Memoria y mapa geológico de España a escala 1:50.000. Hoja de Alpuente (638). Ministerio de Industria, Instituto Geologico y Minero de España (IGME), Madrid.
IGME, 1977. Memoria y mapa geológico de España a escala 1:50.000. Hoja de Jérica (639). Ministerio de Industria, Instituto Geologico y Minero de España (IGME), Madrid.
IGME, 1978. Memoria y mapa geológico de España a escala 1:50.000. Hoja de Camarena de la Sierra (613). Ministerio de Industria, Instituto Geologico y Minero de España (IGME), Madrid.
Iríbar, V., Ábalos, B., 2011. The geochemical and isotopic record of evaporite recycling in spas and salterns of the Basque Cantabrian basin, Spain. Applied Geochemistry 26, 1315–1329.
Jaglarz, P., Szulc, J., 2003. Middle Triassic evolution of the Tatricum sedimentary basin: an attempt of sequence stratigraphy to the Wierchowa unit in the Polisch Tatra Mountains. Annales. Societatis Geologorum Poloniae 73, 169–182.
Jahnert, R.J., Collins, L.B., 2012. Characteristics, distribution and morphogenesis of subtidal microbial systems in Shark Bay, Australia. Marine Geology 303, 115–136.
Kendall, C.G.S.C., Skipwith, P.A., 1968. Recent algal mats of a Persian Gulf lagoon. Journal of Sedimentary Petrology 38, 1040–1058.
Knaust, D., 1998. Trace fossils and ichnofabrics on the Lower Muschelkalk carbonate ramp (Triassic) of Germany: tool for high-resolution sequence stratigraphy. Geologische Rundschau 87, 21–31.
Knaust, D., 2000. Signatures of tectonically controlled sedimentation in Lower Muschelkalk carbonates (Middle Triassic) of the Germanic Basin. In: Bachmann, G.H., Lerche, I. (Eds.), Epicontinental Triassic. Zentralblatt für Geologie und Paläontologie vol. 1, pp. 893–924.
Knaust, D., 2007. Invertebrate trace fossils and ichnodiversity in shallow-marine carbonates of the German Middle Triassic (Muschelkalk). In: Bromley, R.G., Buatois, L.A., Ma'ngano, M.G., Genise, J.F., Melchor, R.N. (Eds.), Sediment-Organism Interactions: A Multifaceted Ichnology. Society of Economic Petrologists and Mineralogists, Special Publications vol. 88, pp. 223–240.
Knaust, D., Costamagna, L.G., 2012. Ichnology and sedimentology of the Triassic carbonates of North-west Sardinia, Italy. Sedimentology 59, 1190–1207.
Koehrer, B.S., Heymann, C., Prousa, F., Aigner, T., 2010. Multiple-scale facies and reservoir quality variations within a dolomite body: outcrop analog study from the Middle Triassic, SW German Basin. Marine and Petroleum Geology 27, 386–411.
Kolar-Jurkovsek, T., Hrvatovic, H., Aljinovic, D., Nestell, G.P., Jurkovsek, B., Skopljak, F., 2021. Permian-Triassic biofacies of the Teocak section, Bosnia and Herzegovina. Global and Planetary Change 200, 103458. https://doi.org/10.1016/j.gloplacha.2021.103458.
Kreisa, R.D., 1981. Storm-generated sedimentary structures in subtidal marine facies with examples from the Middle and Upper Ordovician of southwestern Virginia. Journal of Sedimentary Petrology 51, 823–848.
Lazo, D.G., 2007. Análisis de biofacies y cambios relativos del nivel del mar en el Miembro Pilmatué de la Formación Agrio, Cretácico Inferior de cuenca Neuquina, Argentina. Ameghiniana (Rev. Asoc. Paleontol. Argent.) 44, 73–89.
López-Gómez, J., Arche, A., 1992a. Las unidades litoestratigráficas del Pérmico y Triásico inferior y medio en el sector SE de la Cordillera Ibérica. Estudios Geológicos 48, 123–143 (in Spanish with English abstract).
López-Gómez, J., Arche, A., 1992b. Paleogeographical significance of the Röt (Anisian, Triassic) Facies (Marines clays, muds and marls Fm.) in the Iberian ranges, eastern Spain. Palaeogeography, Palaeoclimatology, Palaeoecology 91, 347–361.
López-Gómez, J., Arche, A., 1994. El Triásico y Pérmico del SE de la Cordillera Ibérica. III Coloquio de Estratigrafía y Paleogeografía del Pérmico y Triásico España, Cuenca. Excursion Guide-book (70 pp., in Spanish).
López-Gómez, J., Arche, A., Calvet, F., Goy, A., 1998. Epicontinental marine carbonate sediments of the Middle and Upper Triassic in the westernmost part of the Tethys Sea, Iberian Peninsula. Zentralblatt für Geologie und Paläontologie 1 (9-10), 1033–1084 (Stuttgart).
López-Gómez, J., Arche, A., Pérez-López, A., 2002. Permian and Triassic. In: Gibbons, W., Moreno, T. (Eds.), The Geology of Spain. Geological Society of London, Special Publication, pp. 185–212.
Mac-Lane, M., 1995. Sedimentology. Oxford University Press, Oxford (423 pp.).
Márquez-Aliaga, A., Ros, S., 2003. Associations of bivalves of Iberian Peninsula (Spain): Ladinian. Albertiana 28, 85–89.

Matysik, M., 2019. High-frequency depositional cycles in the Muschelkalk (Middle Triassic) of southern Poland: origin and implications for Germanic Basin astrochronological scales. Sedimentary Geology 383, 159–180. https://doi.org/10.1016/j.sedgeo.2019.02.001.

Mercedes-Martín, R., Salas, R., Arenas-Abad, C., 2013a. Facies heterogeneity and depositional models of a Ladinian (Middle Triassic) microbial-dominated carbonate ramp system (Catalan Coastal Ranges, NE Spain). Marine and Petroleum Geology 46, 107–128.

Mercedes-Martín, R., Salas, R., Arenas-Abad, C., 2013b. Microbial-dominated carbonate platforms during the Ladinian rifting: sequence stratigraphy and evolution of accommodation in a fault-controlled setting (Catalan Coastal Ranges, NE Spain). Basin Research 26 (2), 269–296.

Myrow, P.M., 1991. Bypass-zone tempestite facies model and proximality trends for an ancient muddy shoreline and shelf. Journal of Sedimentary Petrology 62, 99–115.

Nichols, G., 2009. Sedimentology and Stratigraphy. 2nd ed. Wiley-Blackwell, United Kingdom, p. 419.

Noack, V., Schroeder, J.H., 2003. Porosity development and distribution in the R-dersdorfer Schaumkalk (Middle Triassic) of the Gas Store Berlin, Germany. Facies 48, 255–266.

Ortí, F., Guimerà, J., Götz, A., 2020. Middle–Upper Triassic stratigraphy and structure of the Alt Palància (eastern Iberian Chain): a multidisciplinary approach. Geologica Acta 18 (4), 1–25.

Ortí, F., Pérez-López, A., García-Veigas, J., Rosell, L., Cendón, D.I., Pérez-Valera, F., 2014. Sulfate isotope compositions (δ34S, δ18O) and strontium isotopic ratios (87Sr/86Sr) of Triassic evaporites in the Betic Cordillera (SE Spain). Revista. Sociedad Geologica de España 27, 79–89.

Ortí, F., Pérez-López, A., Salvany, J.M., 2017. Triassic evaporites of Iberia: sedimentological and palaeogeographical implications for the western Neotethys evolution during the Middle Triassic–Earliest Jurassic. Palaeogeography, Palaeoclimatology, Palaeoecology 47, 157–180.

Ortí, F., Salvany, J.M., Rosell, L., Castelltort, X., Inglès, M., Playà, E., 2018. Middle Triassic evaporite sedimetation in the Catalan basin: implications for the palaeogeographic evolution in the NE Iberian platform. Sedimentary Geology 374, 158–178.

Paul, J., Peryt, T.M., 2000. Kalkowsky's stromatolites revisited (Lower Triassic Buntsandstein, Harz Mountains, Germany). Palaeogeography, Palaeoclimatology, Palaeoecology 161, 435–458.

Pérez-Arlucea, M., 1991. Características de los sedimentos carbonáticos de la segunda transgresión del Triásico medio (Ladiniense) en la zona central de la Cordillera Ibérica. Revista de la Sociedad Geológica de España 4, 143–164 (in Spanish with English abstract).

Pérez-Arlucea, M., Rey, D., 1994. Sedimentación continental y marina del Pérmico y Triásico en la zona central de la cuenca Ibérica. Región de Albarracín-El Pobo de Dueñas. III Coloquio de Estratigrafía y Paleogeografía del Pérmico y Triásico España, Cuenca. Excursion Guide-book. p. 56 (in Spanish).

Pérez-López, A., 2001. Significance of pot and gutter casts in Middle Triassic carbonate platform, Betic Cordillera, southern Spain. Sedimentology 48, 1371–1388.

Pérez-López, A., Fernández, J., Solé de Porta, N., Márquez Aliaga, A., 1991. Bioestratigrafía del Triásico de la Zona Subbética (Cordillera Bética). Revista Española de Paleontología, Nº Extraor, pp. 139–150 (in Spanish with English abstract).

Pérez-López, A., Pérez-Valera, F., 2012. Tempestite facies models for the epicontinental Triassic carbonates of the Betic Cordillera (southern Spain). Sedimentology 59, 646–678. https://doi.org/10.1111/j.1365-3091.2011.01270.x.

Pérez-López, A., Pérez-Valera, F., Pérez-Valera, J.A., 2011. Complex palaeogeography of the epicontinental carbonate platform in southern Spain during the Ladinian. Abstract, 28th IAS Meeting of Sedimenology, Zaragoza, Spain, p. 242.

Pérez-Valera, F., Pérez-López, A., 2008. Stratigraphy and sedimentology of Muschelkalk carbonates of the Southern Iberian Continental Palaeomargin (Siles and Cehegín Formations, Southern Spain). Facies 54, 61–87.

Pöppelreiter, M., 2002. Facies, cyclicity and reservoir properties of the Lower Muschelkalk (Middle Triassic) in the NE Netherlands. Facies 46, 119–132.

Pratt, B.R., James, N.P., 1986. The St. George Group (Lower Ordovician) of western Newfoundland: tidal Xat island model for carbonate sedimentation in shallow epeiric seas. Sedimentology 33, 313–344.

Rambaud, D., 1962. Descripción geológica de la región de Tuéjar (Valencia). Madrid, Boletín Instituto Geológico Minero España. vol. 73, pp. 373–418 (in Spanish with English abstract).

Rameil, N., Götz, A.E., Feist-Burkhardt, S., 2000. High-resolution sequence interpretation of epeiric shelf carbonates by means of palynofacies analysis: an example from the Germanic Triassic (Lower Muschelkalk, Anisian) of East Thuringia, Germany. Facies 43, 123–144.

Ramón, X., Calvet, F., 1987. Estratigrafía y sedimentología del Muschelkalk inferior del dominio Monrserrat-Llobregat (Catalanides). Estudios Geológicos 43, 471–487 (in Spanish with English abstract).

Read, J.F., 1985. Carbonate platform facies models. American Association of Petroleum Geologists Bulletin 69, 1–21.

Reading, H.G. (Ed.), 1996. Sedimentary Environments: Processes, Facies and Stratigraphy, 3rd edition Blackwell Science, Oxford, p. 704.

Ricken, W., Eder, W., 1991. Diagenetic modification of calcarous beds - an overview. In: Einsele, G., Ricken, W., Seilacher, A. (Eds.), Cycles and Events in Stratigraphy. Springer-Verlag, Berlin, Heidelberg, pp. 430–449.

Sánchez-Moya, Y., Herrero, M.J., Sopeña, A., 2016. Strontium isotopes of a marine Triassic succession (upper Ladinian) of the westernmost Tethys, Spain. Journal of Iberian Geology 42, 171–186.

Shinn, E.A., 1983. Tidal Xat environment. In: Scholle, P.A., Bebout, D.G., Moore, C.M. (Eds.), Carbonate Depositional Environments. American Association of Petroleum Geologists Memoir vol. 33, pp. 172–210.

Sopeña, A., López-Gómez, J., Arche, A., Pérez-Arlucea, M., Ramos, A., Virgili, C., Hernando, S., 1988. Permian and Triassic basins of the Iberian península. In: Manspeizer, W. (Ed.), Triassic–Jurassic Rifting. Continenal Breakup and the Origin of the Atlantic Ocean and Passive Margins, Part B. Developments in Geotectonics vol. 22, pp. 758–785.

Sopeña, A., Virgili, C., Arche, A., Ramos, A., Hernando, S., 1983. El Triásico. In: Comba, J. (Ed.), Geología de España, t. 2. IGME, Madrid, pp. 47–64 (in Spanish).

Szulc, J., 1997. Middle Triassic (Muschelkalk) sponge-microbial stromatolites, diplopores and Girvanella-oncoids from the Silesian Cracow Upland. 3rd Regional Symp. of International Fossil Algae Association and 3rd International. Meeting of IGCP 380, Guidebook and Abstracts, Cracow, pp. 10–15.

Szulc, J., 1999. Anisian–Camian evolution o f the Germanie basin and its eustatic, tectonic and climatic controls. In: Bachmann, G.H., Lerche, I. (Eds.), Epicontinental Triassic. Zentralblat fur Geologie und Palaeontologie vol. 1, pp. 813–852.

Szulc, J., 2000. Middle Triassic evolution of the Northern Peri-Tethys area as influenced by early opening of the Tethys Ocean. Annates Societatis Geologorum Poloniae 70, 1–48.

Utrilla, R., Pierre, C., Ortí, F., Pueyo, J.J., 1992. Oxygen and sulfur isotope composition as indicators of the origin of the Mesozoic and Cenozoic evaporites from Spain. Chemical Geology 102, 229–244.

Van Wagoner, J.C., Mitchum, R.M., Campion, K.M., Rahmanian, V.D., 1990. Siliciclastic sequence stratigraphy in well logs, cores, and outcrops. Methods in Exploration Series. vol. 7. American Association of Petroleum Geologists (55 pp.).

Vecsei, A., Duringer, P., 1998. Problematic calcispheres from the Upper Muschelkalk (Middle Triassic) of eastern France as producers of calcisiltite and micrite in shallow-water limestones. Paläontologische Zeitschrift 72, 31–39.

Vecsei, A., Duringer, P., 2003. Sequence stratigraphy of Middle Triassic carbonates and terrigenous deposits (Muschelkalk and Lower Keuper) in the SW Germanic Basin: maximum flooding versus maximum depth in intracratonic basins. Sedimentary Geology 160, 81–105. https://doi.org/10.1016/S0037-0738(02)00337-8.

Virgili, C., 1958. El Triásico de los Catalánides. Boletín. Instituto Geológico y Minero de España 69 (856 pp., in Spanish with English abstract).

Virgili, C., Sopeña, A., Ramos, A., Hernando, S., 1977. Problemas de la cronoestratigrafía del Trías en España. Cuadernos Geologí 4, 57–88 (in Spanish).

Walter, M.R., 1976. Stromatolites. Developments in Sedimentology vol. 20. Elsevier, Amsterdam (790 pp.).

Wignall, P.B., Twitchett, R.J., 1999. Unusual intraclastic limestones in Lower Triassic carbonates and their bearing on the aftermath of the end-Permian mass extinction. Sedimentology 46, 303–316.

Zamora, S., Aurell, M., Veitch, M., Saulsbury, J., López-Horgue, M.A., Ferratges, F.A., Arz, J.A., Baumiller, T.Z., 2018. Environmental distribution of post-Palaeozoic crinoids from the Iberian and south-Pyrenean basins, NE Spain. Acta Palaeontologica Sinica 63 (4), 779–794. https://doi.org/10.4202/app.00520.2018.

Zhang, X.Y., Wang, W.Q., Yuan, D.X., Zhang, H., Zheng, Q.F., 2019. Stromatolite-dominated microbialites at the Permian–Triassic boundary of the Xikou section on South Qinling Block, China. Palaeoworld 29, 126–136. https://doi.org/10.1016/j.palwor.2019.05.009.

Ziegler, P.A., 1982. Triassic rifts and facies patterns in Western and Central Europe. Geologische Rundschau 71, 747–772.

Ziegler, P.A., 1988. Post-Hercynian plate reorganization in the Tethys and the Artic-North Atlantic domains. Developments Geotectonics vol. 22B. Elsevier, pp. 156–711.

Zwenger, W.H., 1993. Die Schichtenfolge Muschelkalk einschlieβlich Röt. In: Schörder, J.H. (Ed.), Die Struktur Rüdersdorf. Fihrer zur Geologie von Brandenburg vol. 1, pp. 37–66.